Aus dem

Department für Augenheilkunde Tübingen

Universitäts-Augenklinik

In Vitro Evaluation of Lymphocyte Viability Following Vitrectomy: Implications for Ocular Lymphoma Biopsy Techniques

Inaugural-Dissertation
zur Erlangung des Doktorgrades
der Medizin

der Medizinischen Fakultät
der Eberhard Karls Universität
zu Tübingen

vorgelegt von

Kowalski, Martin

2025

Dekan: Professor Dr. B. Pichler

1. Berichterstatter: Professor Dr. K. U. Bartz-Schmidt
2. Berichterstatter: Professor Dr. F. Fend

Tag der Disputation: 28.11.2025

Table of contents

List of figures

List of tables

Abbreviations

LIST OF ABBREVIATIONS AND ACRONYMS

A	area
APC-Cy7	allophycocyanin - cyanine 7
BCR	B-cell receptor
BSC	biological safety cabinet
cfDNA	cell-free DNA
CNS	central nervous system
CO_2	carbon dioxide
cpm	cuts per minute
ctDNA	circulating tumor DNA
ddPCR	digital droplet PCR
DLBCL	diffuse large B-cell lymphoma
DNA	desoxyribonucleic acid
EDTA	ethylenediaminetetraacetic Acid
EMZL	extra nodal marginal zone lymphomas
ETS	E-twenty-six transcription factor family
ETV6	ETS Variant Transcription Factor 6
FA	fluorescence angiography
FACS	fluorescence-activated cell sorting
FCS	foetal calf serum
FSC	forward scatter
g	gravity
G	gauge
H	height
HOPE	Hepes Glutamic Acid Buffer Mediated Organic Solvent Protection Effect
IGLL5	immunoglobulin lambda-like polypeptide 5
IHL	immunoglobulin heavy locus
M	molar
MALT	mucosa-associated lymphoid tissue
MIVS	microincision vitrectomy surgery
mL	milliliter
mM	millimolar
MYD88	myeloid differentiation primary response 88
NF-κB	nuclear factor kappa-light-chain-enhancer of activated B cells
NGS	next generation sequencing
OCT	optic coherence tomography
PBMC	peripheral blood mononuclear cell
PBS	phosphate-buffered saline
PCNSL	primary central nervous system lymphoma
PCR	polymerase chain reaction
PIM1	proviral integration site for Moloney murine leukemia virus 1
PIOL	primary intraocular lymphoma
PPV	pars-plana vitrectomy
PVRL	primary vitreoretinal lymphoma
RPMI	Roswell Park Memorial Institute 1640 culture medium

SSC	side scatter
TDC	two-dimensional cutting
TMD8	Tokyo Medical and Dental University 8 cell line
VRL	vitreoretinal lymphoma
VR-LBCL	vitreoretinal large b-cell lymphoma
W	width
9p21/CDKN2A	cyclin-dependent kinase inhibitor 2A

1 Introduction

1.1 Anatomic background and ocular lymphatic tissues

The vitreous body and its adjacent retina are a sophisticated anatomical region characterized by complicated tissue interactions. (Sebag, 2016) The vitreous humor, a transparent gel-like substance, lies in the posterior chamber of the eye and provides the structural support of the retina, while also maintaining optical clarity (Sebag, 1987). The retina, a multilayered neurosensory tissue, contains the photoreceptor cells and complex neural structures that facilitate visual signal transduction. (Snell & Lemp, 2013) Like the CNS the internal tissues of the eye do not possess any lymphatics or lymph nodes. The lymphatic drainage of the eye occurs primarily through the uveoscleral pathway and episcleral lymphatic vessels, which facilitate immune cell migration and contribute to maintaining immunological homeostasis in this delicate anatomical region. (Levin et al., 2011)

Immunohistological studies though have suggested a lymphocytic microenvironment, the so called ‘glymphatic system’ (Iliff et al., 2012) within the vitreous and retinal tissues, with resident and infiltrating immune cells such as macrophages, T-lymphocytes, and dendritic cells playing critical roles in immune surveillance and inflammatory responses. (Denniston & Keane, 2015; Uddin & Rutar, 2022) It is therefore hypothesized, that vitreoretinal lymphomas (VRL) arises from lymphocytes that normally travel through the CNS or form a pathological cell that homes into the CNS. (Singh & Damato, 2019)

1.2 Tumorous transformation and the development of B-cell lymphoma

B-cell lymphomas are a diverse group of malignancies originating from B lymphocytes. They arise through a complex interplay of genetic mutations and microenvironmental factors (Küppers, 2005; Young et al., 2019). The transformation of these neoplasms begins with genetic damage during the germinal center reaction, a process, which is crucial for antibody diversification (Shaffer et al., 2012). This damage leads to chromosomal translocations,

oncogenic mutations, and epigenetic modifications that disrupt normal B-cell signalling pathways and regulatory mechanisms (Thurner et al., 2020).

An important event in lymphoma development is the subversion of B-cell receptor (BCR) signaling, which malignant cells use to sustain their growth and survival (Küppers, 2005; Young et al., 2019). The mechanisms facilitating this transformation include chromosomal translocations, which can create oncogenic fusion proteins, and epigenetic changes that alter gene expression without modifying the DNA sequence (Thurner et al., 2020).

The tumor microenvironment plays a critical role in modulating anti-tumor responses, promoting an environment, which is conducive to lymphoma progression supporting the survival and proliferation of malignant B cells (Seifert et al., 2013; Touitou et al., 2007; Young et al., 2019).

1.3 Vitreoretinal Lymphoma

1.3.1 Classification of vitreoretinal lymphomas

The term “primary intraocular lymphoma” (PIOL) as described by Cooper & Riker in the fifties (Cooper & Riker, 1951; Qualman et al., 1983) has been replaced by a more specific terminology due to distinctive anatomical and histological features of lymphomas originating from the uveal tract versus entities originating from the retina or vitreous body (Coupland et al., 2009). Unlike VRL, uveal and choroidal lymphomas are most commonly low-grade extranodal marginal zone lymphomas (EMZL) of the mucosa-associated lymphoid tissue (MALT) type (Coupland & Damato, 2008; Coupland et al., 2004).

Vitreoretinal lymphomas are generally categorized as primary vitreoretinal lymphomas (PVRL), which arise in the ocular tissues and as such are a variant of the primary central nervous system lymphoma (PCNSL) with no systemic involvement, or secondary vitreoretinal lymphomas, which are a metastasized through hematogenous dissemination from a systemic primary lymphoma (Giuffrè et al., 2020; Sobolewska et al., 2021).

Histologically, VRL are divided into diffuse large B-cell lymphoma (DLBCL), which is the most common subtype of VRL, mediastinal large B-cell lymphoma, and other rare types such as Burkitt's lymphoma or T-cell lymphoma, which are less commonly reported (Alaggio et al., 2022).

Immunophenotypically, genetically and based on the mutation profile, VRL usually (in 95%) belongs to the type of diffuse large B-cell lymphoma, which is the most common form of non-Hodgkin's lymphoma (Alaggio et al., 2022). The exact cellular derivation however remains debatable. Some studies suggest an origin from early post-germinal center B-cells due to highly somatically mutated IGH genes, while others indicate a germinal center B-cell origin for a subgroup of these lymphomas, which may be associated with a better prognosis (Coupland et al., 2009; Fend et al., 2016).

Recent NGS genomic studies of vitreous samples identified VRL as part of the *MYD88*/*CD79B*-mutated (MCD) or cluster 5 subgroup of DLBCL with percentages ranging from 74% (Bonzheim et al., 2015; Bonzheim et al., 2022) up to a substantial 91% (Kwak et al., 2023) of *MYD88* mutations in the samples.

Both primary and secondary VRLs however show a similar genetic profile, indicating that secondary spread to the vitreoretinal space might be causally connected to its biological properties rather than by chance alone (Arai et al., 2020; Kwak et al., 2023). Further mutations commonly occur in the *9p21/CDKN2A*, *PIM1*, *IGLL5* and *ETV6* genes (Bonzheim et al., 2022).

1.3.2 Vitreoretinal lymphoma

VRL is a rare and aggressive malignancy most commonly originating from B lymphocytes, primarily affecting the retina, vitreous, and central nervous system (CNS). As a subset of primary CNS lymphoma (PCNSL), VRL is predominantly classified as diffuse large B-cell lymphoma (DLBCL) (Androudi et al., 2024; Sobolewska et al., 2021). Similar pathophysiological mechanisms as in CNS lymphoma have been shown to be responsible for VRL development (Touitou et al., 2007). This intraocular malignancy poses significant diagnostic challenges due to its nonspecific presentation, often mimicking chronic uveitis, which can lead to substantial delays in diagnosis (Giuffrè et al., 2020).

1.3.3 Epidemiology

With 0.047 cases per 100,000 people per year (Levasseur et al., 2013), it is responsible for 4% to 6% of all brain tumors and less than 1% of all non-Hodgkin lymphomas (Venkatesh et al., 2019). Although the real incidence in the population is probably underestimated and still not fully documented, within the last decades the prevalence seems to increase worldwide but nevertheless remains a rare ocular disease (Levasseur et al., 2013; Sjö, 2009; Sobolewska et al., 2021). Recent studies suggest a higher incidence (1:100000) with 80% CNS involvement (Menean et al., 2023) as clinical suspicion and diagnostic methods improve.

VRL typically manifests bilaterally, with approximately 65% of cases presenting in both eyes at onset (Androudi et al., 2024). The disease carries a poor prognosis, with roughly half of all affected patients developing CNS involvement (Singh & Damato, 2019).

Vitreoretinal lymphoma is more common in the elderly, particularly in people with immunosuppression (Cassoux et al., 2000; Sobolewska et al., 2021). Recent data shows a higher prevalence in women with some studies suggesting a 2:1 ratio (Alfaar et al., 2024; Venkatesh et al., 2019).

The 5-year survival is estimated to be at 41% and 30%, with median survival of 3.2 and 2.1 years based on retrospective data from the United States National Cancer Institute and the Australian Cancer Database, respectively (Ahmed et al., 2017; Farrall & Smith, 2023).

1.3.4 Clinical presentation

Patients typically present with gradual onset of nonspecific symptoms, such as painless moderate blurred vision, floaters, and ocular discomfort often masquerading as chronic or relapsing uveitis (Sobolewska et al., 2021).

Clinically the funduscopic examination may show the presence of vitreous opacities, more specifically numerous vitreous cell sheets, which are larger but less dense than those seen in vitritis. Other findings may include multifocal yellowish-white or cream-colored subretinal or retinal lesions, observed in approximately 50% of cases at presentation (Menean et al., 2023; Sobolewska et al., 2021). Visual acuity often remains better than expected in view of the significant vitreous haze due to the lack of macular edema (Chan et al., 2011).

The masquerading of a chronic or relapsing uveitis with blurred vision, floaters and intraocular infiltration makes a clinical diagnosis challenging (Cao et al., 2011; Melli et al., 2022; Takase et al., 2022). These nonspecific findings, coupled with a partial response to local and occasionally systemic steroids—commonly used as first-line management in suspected uveitis cases—frequently result in misdiagnosis and treatment delays. Consequently, central nervous system involvement may develop in up to 80% of patients within one year (Giuffrè et al., 2020; Menean et al., 2023).

Therefore, suspicion should be raised when the age of onset is over 60 years, a nearly preserved visual acuity despite dense vitreous opacities with cells and subretinal infiltration and a lack of macular edema can be observed (Chan et al., 2011). Furthermore, a classic, however often not distinct, finding for choroidal lymphoma is a leopard patterning in fundoscopy and fluorescence angiography (Fardeau et al., 2009).

1.3.5 Challenges in VRL diagnosis

VRL represents one of the most challenging ocular conditions to manage for clinicians, due to ambiguous symptoms and furthermore due to the lack of standardized guidelines for diagnosis, treatment, and follow-up. Its rarity often leads to misdiagnosis, resulting in several months or years of diagnostic delay. Clinical findings are rarely specific, masquerading as posterior or intermediate uveitis of other etiologies.

Recent advancements in eye imaging modalities like widefield color fundus photography, fluorescein angiography (FA), and optical coherence tomography

(OCT) have allowed for the identification of typical lymphoma features. However, diagnosis of certainty still requires invasive vitreoretinal biopsy.

Cytology specimens have been shown to generate false-negative results in a consistent percentage of analyses. The causes for such a high rate of false negatives include the paucity and fragility of lymphomatous cells in the sample, and the cytopathologist's experience. Recently, new techniques have been established to increase the predictive value of PVRL diagnosis, such as the detection of the mutation *L265P* in the gene *MYD88* (highly specific for large B-cell lymphomas) in ocular fluids like the aqueous and vitreous humor.

The gold standard for diagnosis, cytological analysis of vitreous samples, often has been hampered by the low cell counts in samples with low vitreous biopsy volumes and the high fragility of lymphoma cells, which are often degraded by prior steroid treatment for presumed uveitis (Coupland, 2012; Melli et al., 2022). These factors resulted in low diagnostic sensitivity of cytological examinations alone (Takase et al., 2022). Additionally, the lack of standardized diagnostic criteria and the need for specialized expertise in interpreting vitreous cytology samples further complicated the diagnostic process (Levasseur et al., 2013). These challenges often necessitated multiple vitreous biopsies, increasing the risk of complications and delaying definitive diagnosis, potentially allowing for disease progression and poorer outcomes (Dalal et al., 2014; Dawson et al., 2018; Soussain et al., 2021). Not infrequently even retinal biopsies within the setting of a vitrectomy are necessary.

1.3.6 Diagnostics

A diagnostic pars plana vitrectomy with removal of a vitreous sample for a subsequent histopathological analysis is still the gold standard in diagnosis (Gonzales & Chan, 2007). Literature reports the sensitivity of vitrectomy to be 77% and the specificity to be 73% (Almeida et al., 2016).

1.3.6.1 Cytology

Cytopathological examination of vitreous samples obtained through pars-plana vitrectomy remains the gold standard for diagnosing vitreoretinal lymphoma (VRL). This technique involves the microscopic evaluation of cellular components present in the vitreous humor, allowing for the identification and characterization of malignant lymphoid cells.

The cytological features of VRL typically include large atypical lymphoid cells with prominent nucleoli, irregular nuclear contours, and scant cytoplasm. These cells often demonstrate a high nuclear-to-cytoplasmic ratio and may exhibit mitotic figures (Melli et al., 2022). However, the diagnostic yield of cytological analysis can be variable, ranging from 45% to 60%, due to several factors: Vitreous samples often contain a limited number of cells, making diagnosis challenging. Lymphoma cells are prone to degradation during sample processing. Corticosteroid therapy, often administered before diagnosis, can lead to cell lysis and compromise cytological evaluation (Choo et al., 2024).

To enhance diagnostic accuracy, cytological examination is frequently complemented by immunophenotyping techniques such as flow cytometry and immunohistochemistry. These methods allow for the detection of specific cell surface markers characteristic of B-cell lymphomas, including CD19, CD20, and CD79a (Coupland et al., 2004).

Recent advancements in cytological techniques have improved diagnostic yield. The cell block technique, which involves embedding cellular material in paraffin, allows for better preservation of cellular morphology and enables additional immunohistochemical staining (Kwak et al., 2023). Moreover, the application of cytospin preparations has shown promise in increasing cellular yield and improving morphological assessment (Bonzheim et al., 2022).

1.3.6.2 Liquid biopsy and next-generation sequencing

The advent of liquid biopsy techniques and next-generation sequencing (NGS) has revolutionized the molecular diagnosis of VRL, offering a less invasive and more comprehensive approach to disease characterization.

Liquid biopsy in VRL involves the analysis of cell-free DNA (cfDNA) and circulating tumor DNA (ctDNA) present in ocular fluids, primarily the vitreous humor and aqueous humor. This approach allows for the detection of specific genetic alterations associated with VRL without the need for cellular material (Tan et al., 2020).

NGS technologies have enabled the identification of recurrent genetic mutations in VRL, providing valuable diagnostic and prognostic information. The most frequent mutations observed in VRL include *MYD88 L265P, CD79B, PIM1, BTG2*, and *TBL1XR1* (Menean et al., 2023). *MYD88* is present in up to 80% of VRL cases. This mutation activates the NF-κB pathway and is highly specific for VRL (Bonzheim et al., 2022; Cani et al., 2017). *CD79B* mutations often co-occur with *MYD88* mutations and are found in approximately 40% of VRL cases (Bonzheim et al., 2023).

The application of targeted NGS panels focusing on these recurrently mutated genes has significantly improved the diagnostic accuracy of VRL. A recent study by Bonzheim et al. (2022) demonstrated that NGS-based mutation profiling could detect VRL with a sensitivity of 85% and a specificity of 100%.

Furthermore, liquid biopsy combined with digital droplet PCR (ddPCR) has shown promise in monitoring treatment response and detecting minimal residual disease in VRL patients. This highly sensitive technique can detect mutant alleles at frequencies as low as 0.1%, allowing for early detection of disease recurrence (Hiemcke-Jiwa et al., 2018).

The integration of these molecular techniques with traditional cytopathology has led to a paradigm shift in VRL diagnosis. A multi-modal approach combining

cytology, immunophenotyping, and molecular analysis now represents the optimal diagnostic strategy for VRL, significantly reducing time to diagnosis and improving patient outcomes (Hiemcke-Jiwa et al., 2018; Huang et al., 2024).

While cytopathological analysis remains fundamental in VRL diagnosis, the incorporation of advanced molecular techniques such as liquid biopsy and NGS has markedly enhanced our ability to detect and characterize this challenging malignancy. These innovations not only improve diagnostic accuracy but also provide insights into disease biology and potential therapeutic targets, paving the way for personalized treatment approaches in VRL.

1.3.6.3 Vitreous biopsy

The procedure for vitreous biopsy typically involves pars plana vitrectomy (PPV) or only vitreous aspiration. PPV is generally preferred in Europe as it allows for the collection of a larger sample volume (50-100 ml of diluted vitrectomy cassette fluid) compared to vitreous aspiration (1-2 ml of undiluted specimen) (Venkatesh et al., 2019).

Since Machemer developed the first 17 G vitrectomy in the 1970s the systems were revolutionized. Newer systems came with more stable flows and dynamics (de Oliveira et al., 2016).

When deciding for the right lumen diameter, there is always a trade-off between the durability and flexibility of the instruments, pace of vitreous removal and wound management. The larger the gauge diameter the larger amount of vitreous a cutter can remove per time. But a greater diameter results in risking an expanded wound leakage, hypotony and infection (Pandit et al., 2023). The evolution of minimally invasive techniques, such as 23-, 25-, and 27-gauge systems, has improved the safety and efficacy of vitreoretinal procedures (Ribeiro et al., 2022; Tang et al., 2020). Small-gauge vitrectomy presents distinct advantages over conventional 20-gauge instrumentation in the treatment of retinal diseases. These benefits include easier insertion into the anterior chamber to remove pupillary membranes, reduced post-operative inflammatory irritation, and overall shorter operating times (Lee et al., 2022; Mahajan et al., 2011;

Mohamed et al., 2017; Tarantola et al., 2012). Small-gauge transconjunctival sutureless vitrectomy, particularly utilizing 25G or 27G instrumentation, has proven to be a safe and effective technique for diagnosing vitreoretinal lymphoma (Tan et al., 2020). The choice of instruments and gauge diameter should be adapted to the specific clinical case. While smaller gauge instruments offer numerous advantages, they may sometimes provide a lower diagnostic yield compared to larger gauge instruments due to the reduced flow rates and smaller port sizes (Menean et al., 2023). Therefore, the surgeon must balance the benefits of minimally invasive techniques with the need for adequate sample collection for diagnostic purposes.

Not only the gauge diameter has a paramount share in vitrectomy but cutter designs and cutting rates. Modern systems allow cutting rates up to 20.000 cuts per minute (cpm) or more.

These developments have enabled surgeons to work more precisely while minimizing trauma to the eye. Intraoperative imaging technologies, including optical coherence tomography (OCT), have further enhanced the accuracy of biopsy procedures by providing real-time visualization of retinal structures (Sadeghi et al., 2023). Additionally, the integration of robotic assistance in vitreoretinal surgery shows promise for increasing precision and stability during delicate maneuvers (Roizenblatt et al., 2018). These technological advancements have collectively contributed to more reliable cytologic and molecular diagnostics for VRL (Sobolewska et al., 2021; Tan et al., 2020).

To maximize the cellular yield, a two-step technique is often employed. First, an undiluted vitreous sample (0.5-1 ml) is collected using a syringe attached to the aspiration line of the vitrector, with the infusion turned off. This is followed by a diluted sample collection after the infusion is turned on (Hwang et al., 2014). It is essential to handle the samples with care and transport them to the laboratory promptly, preferably within 30 minutes of collection, to ensure adequate cellular

viability (Venkatesh et al., 2019). Proper handling of the obtained samples is crucial for accurate diagnosis. Samples should be transported to the laboratory without delay and without fixation, or with mild fixatives such as Cytolyt or HOPE solution if immediate processing is not possible (Carbonell et al., 2021). The use of formalin fixation should be avoided as it can compromise cell morphology and immunoreactivity (Tan et al., 2020).

In cases of inconclusive vitreous samples and clear retinal or subretinal lesions, retinal and/or subretinal biopsies may be considered. These can be performed using either a cutting/aspiration technique with a vitreous cutter or a bimanual dissection technique with retinal scissors and forceps (Huang et al., 2024).

By carefully considering these factors and utilizing appropriate techniques, vitreous biopsy can yield valuable diagnostic insights in suspected cases of vitreoretinal lymphoma, thereby informing further management and treatment decisions. While aspiration biopsy suffices for NGS testing of *MYD88*, vitrectomy remains essential since *MYD88* is present in both B-cell lymphomas and low-malignant mantle cell lymphomas. Consequently, additional cytological analysis is crucial for accurate therapeutic decision making.

1.4 Effect of vitrectomy setting on sample quality – previous studies

A comparison of different surgical techniques when performing diagnostic vitrectomies has been carried out in relation to endophthalmitis (Almeida et al., 2016). Comparable results were found for visual acuity in small-gauge vitrectomies (23 and 25 G) compared to 20-gauge instrumentation. However, significant differences in the culture-positive rates of the pathogens were identified. The 20-gauge cohort generated significantly higher culture-positive results (Almeida et al., 2016). In the context of intraocular infections, the diagnostic vitrectomy itself has a curative effect as the small molecules of inflammatory agents such as interleukins and bacterial deposits are partly wiped out. For 20 G vitrectomy this eradication can be performed more rapidly compared to smaller gauge sizes.

1.4.1 Studies in lymphoma diagnostics

In 2014, Jiang et al. Investigated the effect on higher cutting rates in 20 G vitrectomy for lymphoma cells. This study revealed a decrease in cell viability already above 600 cpm (Jiang et al., 2014).This therapeutic regime was thereafter adopted into recommendations for suspected lymphoma cases to obtain a higher diagnostic yield and more viable lymphoma cells. (Tan et al., 2020).

Vitreous biopsy has also recently been investigated for 25 G with different cutting rates of 500, 1000, 4000, 7500, or 15000 cuts per minute. There was no significant difference in yield for different cutting rates (Tekumalla et al., 2023; Xu et al., 2022). Another case-series documented the cytology results of diagnostic vitrectomies in suspected cases of PVR-LBCL with 25 G and compared these results to literature of 20 G vitrectomies. They found more positive yields in 25 G vitrectomies (Kanavi et al., 2014).

So far there is no systematic evaluation and comparison of biopsy results in all available cutter sizes with different cutting rate settings.

1.5 Study aims

Regarding the delicate nature of the vitreous and the biopsy specimen in VR-LBCL, where the cells are larger in size, more fragile and subsequent histopathology is of decisive importance for the final treatment of the patient, the gauge size and cutting rate during vitrectomy might play a significant role (Tekumalla et al., 2023; Ulltang et al., 2021).

As shown above, there is a need for a standardization of a vitreous biopsy in cases suspicious for malignancy as delaying the diagnosis might have vision and even life-threatening consequences and concise recommendations for a correct vitrectomy technique are missing. Therefore, in this study a model was developed to mimic the cutting and aspiration during vitrectomy and the mechanical impact on the lymphatic cells with different gauge sizes.

We evaluated the impact of vitrectomy on lymphocyte integrity using both healthy human peripheral blood lymphocytes (Kizhakeyil et al., 2019) and cultured *MYD88*-mutated lymphoma cells. In the healthy peripheral lymphocyte cohort a subgroup analysis was performed on peripheral blood mononuclear cells. Standardized cell suspensions ($1x10^3$cells/ml, $1x10^4$cells/ml, and $1x10^6$cells/ml cells/mL) underwent vitrectomy under controlled conditions, with post-procedure viability assessed via flow cytometry.

The primary endpoint was defined as intact cell survival after vitrectomy of standardized cell cultures. Vitrectome diameters of 20G, 23G, 25G and 27G were compared.

Secondary endpoints included the effects of aspiration alone versus two cutting rates (1500 and 5000 cpm), and the influence of initial cell concentration on outcomes.

The results should provide a relevant guidance for the clinical work of vitreoretinal surgeons on the extent to which the cutting rate and the diameter size of the vitrectome have an influence on the integrity of the B lymphocytes and, thus, the proof of suspected vitreoretinal lymphoma cases.

2 Materials and Methods

2.1 Blood Sampling and Lymphocyte Isolation

2.1.1 Sample Collection

After informed consent, one individual served as the blood donor (Fig. 2-1). Blood sampling was performed by a trained clinician using a 21G Safety-Multifly-Canula (Sarstedt, Nümbrecht, Germany) from the antecubital vein. Approximately 100 ml of venous blood was collected into a total of eleven to twelve 9 ml Sarstedt EDTA monovettes (Sarstedt, Nümbrecht, Germany). The blood collection was conducted according to standardized in-house clinical protocols under aseptic conditions. Each monovette was gently inverted multiple times immediately after collection to ensure proper anticoagulant mixing and prevent cellular clumping. The monovettes were immediately transferred to the laboratory for lymphocyte isolation.

2.1.2 Lymphocyte isolation by Ficoll gradient sedimentation

The collected whole blood samples were carefully transferred to 50 ml Falcon tubes and diluted to a minimum of 1:2 with PBS (at room temperature). Per 30 ml of diluted blood product, 15 ml of Ficoll (BioColl® Separation Solution, Bio&Sell, Germany was layered into a 50 ml tube. The blood mixture was gently layered over the Ficoll, maintaining a 45-degree tube angle and using a low-speed pipette setting to create a broad, uninterrupted blood stream.

The Ficoll layered tubes were then centrifuged at 800g for 30 minutes at 21 °C. The PBS and platelet layer was discarded, retaining the lymphocyte ring (approximately 25 ml in the tube).

The lymphocyte layer was carefully removed and transferred to a fresh Falcon tube (maximum 10 ml per tube), diluted with PBS to 50 ml, taking care to minimize Ficoll carryover and not to whirl up any of the lymphocytes. A total of three washing cycles were performed, each one for 10 minutes at 21°C, subsequently lowering gravitational force (G) with every successive centrifugation (500g, 400g, 250g, respectively).

After the final centrifugation, the supernatant was removed, and the cells resuspended into RPMI 1640 Medium with GlutaMAX supplement (Gibco™, Thermo Fisher Scientific, UK) and incubated overnight (at 37°C in an atmosphere of 5% CO2 and 100% humidity).

2.1.3 Preparation of test suspensions

The following morning, cell suspensions with defined concentrations were prepared by utilizing only the supernatant (containing only B-Lymphocytes and PBMCs, while T-lymphocytes settle at the bottom of the vial) and leaving a small residue at the bottom of the container. Concentrations of $1x10^6$/ml, $1x10^4$/ml and $1x10^3$/ml were prepared in 50ml tubes, giving a total volume of 50ml for each concentration. The tubes immediately transferred to the operating room for experimental vitrectomy.

2.2 Cell culture of *MYD88*-positive Lymphoma cells

Commercially bought *MYD88*-positive *TMD8* lymphoma cells (Leibniz Institute DSMZ, RI-1, ACC 585) were cultured in RPMI 1640 medium supplemented with GlutaMAX™ (Gibco™, Thermo Fisher Scientific, UK) to enhance cell viability and growth. Cells were maintained in a humidified incubator at 37°C with 5% CO2 (see section above), and media was refreshed every two to three days to ensure optimal nutrient availability. The culture conditions were monitored regularly, and cell density was adjusted as necessary to prevent over-confluence. For experimental procedures, cells were harvested using trypsin-EDTA and counted using a hemocytometer to ensure accurate cell numbers for preparation of cell suspensions. Again, cell concentrations of $1x10^6$/ml, $1x10^4$/ml and $1x10^3$/ml were prepared in 50ml Falcon tubes, resulting in a total volume of 50ml for each concentration. The tubes were immediately transferred to the operating room for experimental vitrectomy.

2.3 Experimental vitrectomy of cell suspensions

The prepared cell suspensions were immediately transported to the operating room of the Tübingen Eye Clinic, where standardized experimental vitrectomy protocols were performed.

Four different cutter sizes (23G, 25G, and 27G from D.O.R.C.©, Dutch Ophthalmic Research Center, Zuidland, The Netherlands; and 20G from MIDlabs©, Medical Instrument Development Laboratories, Inc., San Leandro, California, United States) were utilized, along with three distinct cutting rates (0cpm, 1500cpm and 5000cpm) for each cell concentration. The experiments were done using Qube™ pro vitrectomy system (Fritz Ruck Ophthalmologische Systeme GmbH, Eschweiler, Germany)

Prior to sampling, the cell suspension was inverted three times to ensure even distribution of cells within the flask. The vitrectomy probe was positioned centrally within the Falcon™ tube, and the cutting speed was adjusted on the vitrectomy device. Initially, only aspiration was performed, with a total volume of 3 ml aspirated using a 5 ml disposable luer lock syringe. The syringe was then sealed with a Combi-Stopper, labeled, and stored at room temperature until the conclusion of the experiment. After removing the probe from the suspension, any excess liquid was discarded. The next cutting rate was set, the Falcon™ tube was inverted three times, and a subsequent sample was collected from the center of the remaining volume. This procedure was repeated for all four vitrectomy probes and all three cell concentrations and both healthy lymphocyte cultures and *MYD88*-positive cell cultures, resulting in a total of 36 processed samples per experiment. Additionally, a residual volume of 9 ml was retained each time in the Falcon™ tube to serve as a control sample without vitrectomy for subsequent cell sorting.

Upon completion of experimental vitrectomies, samples were immediately returned to the laboratory for FACS processing.

2.4 Fluorescence-activated cell sorting (FACS)

Flow cytometry was performed using an LSR Fortessa X20 (BD Biosciences, NJ) at the Clinical Immunotherapy Research Group laboratory of the University Children's Hospital Tübingen.

Cell viability was assessed using the LIVE/DEAD™ Fixable Near IR (780) Viability Kit (Thermo Fisher Scientific) according to the manufacturer's recommended protocol. Briefly, the vitrectomized cells were resuspended in PBS and incubated with the near-infrared fluorescent live/dead reagent for 30 minutes at room temperature, protected from light. The staining reaction was performed at a 1:1000 dilution of the stock dye in PBS. After incubation, the cells were washed twice with cold PBS to remove unbound dye, centrifuged at 400g for 5 minutes at 4°C, and finally resuspended in FACS buffer for subsequent analysis. The near-infrared dye selectively labels membrane-compromised dead cells, allowing for precise discrimination between viable and non-viable cell populations during flow cytometric analysis.

Prior to the sorting process, the flow cytometer was configured with a minimalist parameter setup, retaining only forward scatter (FSC), side scatter (SSC), and APC-Cy7 detectors. Detector settings were standardized by selecting height (H), width (W), and area (A) parameters for FSC and SSC to enable comprehensive cellular characterization.

Initial instrument calibration involved preparing a test sample comprising 1 million isolated cells, washed and resuspended in FACS buffer with negative beads. To ensure accurate compensation for spectral overlap, the AbC™ Total Antibody Compensation Bead Kit was utilized, allowing for precise adjustment of fluorescence signals prior to sample acquisition. A preliminary "Test" tube was created to establish optimal scatter plot configurations. FSC and SSC voltages were adjusted to ensure precise cell and bead population positioning consistent with the predefined experimental schematics.

Initially, a "beads only" control was measured at low or medium sensitivity to establish baseline parameters. The target bead acquisition was set between 15,000-25,000 events within gate P1, with each measurement standardized to approximately 1.5 minutes in duration. To maintain data integrity, proportional event scaling was implemented when suboptimal bead concentrations were detected.

For each experimental series, 44 FACS tubes were meticulously prepared, comprising 39 experimental sample tubes, three untreated control tubes, one heat-treated cell sample, and a negative bead control. Signal optimization was focused on maintaining the APC-Cy7 detector voltage position with positive peaks at 10^5 intensity.

This calibration ensured comprehensive and interpretable data collection across all experimental samples, providing the foundation for subsequent data analysis in FlowJo software V7.6.5 (FlowJo LLC, OR). Measurement strategies were dynamically adapted to maintain consistent cellular event numbers, with bead reference quantities adjusted to target a minimum of 25,000 cell events per sample. In the lymphocyte group a population of peripheral blood mononuclear cells (PBMC) could be identified and singled out.

The whole workflow is illustrated in figure 2-1.

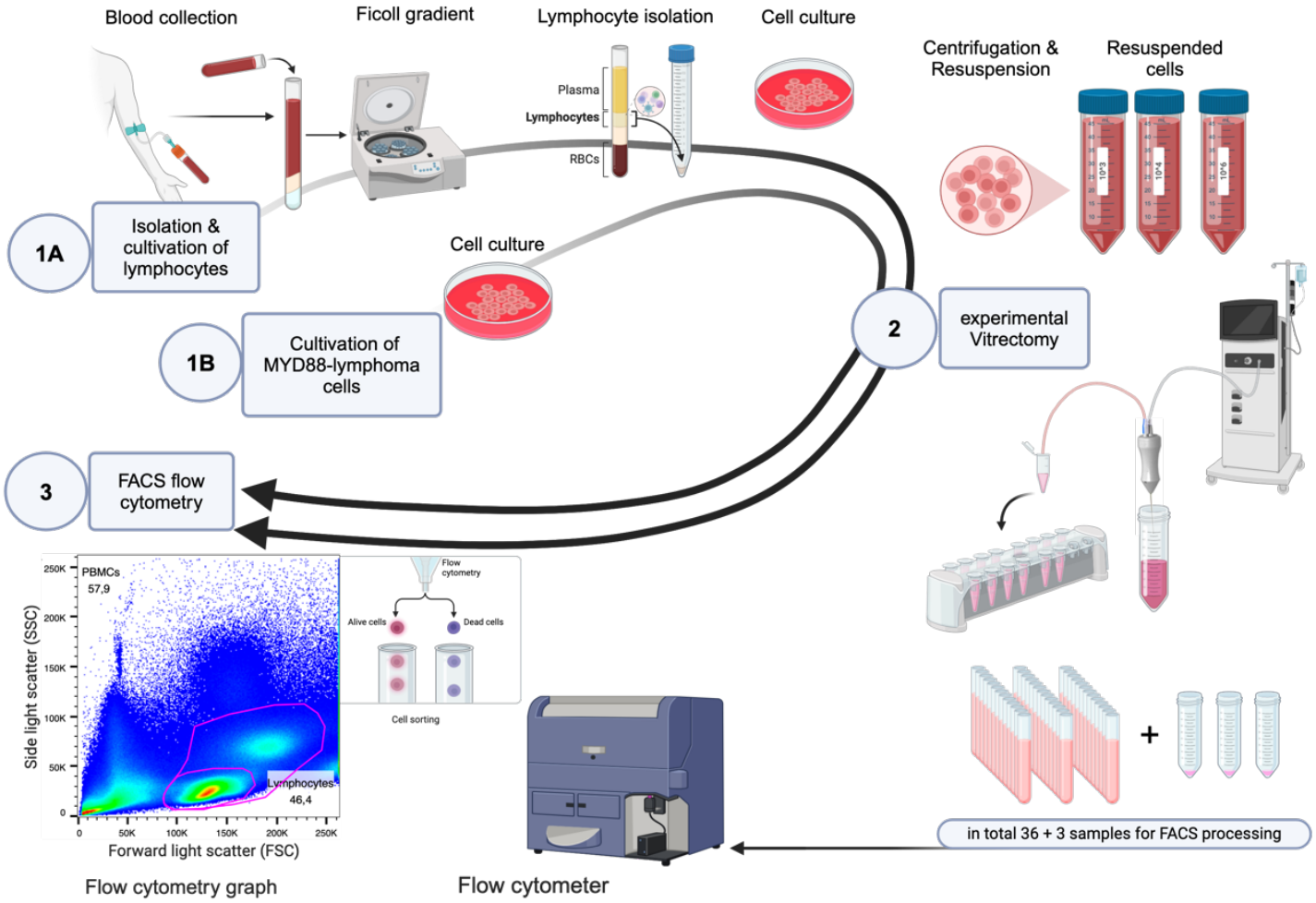

Figure 2-1: Study overview.

2.5 Statistical Analysis

All statistical analyses were conducted using the R statistical language (version 4.3.3; R Core (Team, 2024)) on MacOS Sonoma 14.5., and results are presented as median values with interquartile ranges

To assess the differences in the respective alive cell fractions across different gauge sizes and cutting rates, we employed the Kruskal-Wallis test, a non-parametric method suitable for comparing three or more independent groups. This test was chosen due to the non-normal distribution of our data, as confirmed by the Shapiro-Wilk test. The distribution of the data was evaluated using a combination of graphical and statistical methods. Visual inspection of the data distribution was conducted using histograms, QQ-plots, and scatterplots. Additionally, Kendall correlation coefficients were calculated to assess and confirm the strength and direction of correlations among variables. We used Kendall correlation coefficient because of the ordinal character of the data (Gauge size, cutting rate).

The groups were defined based on cutting rates (0, 1500 and 5000) and gauge numbers (20G, 23G, 25G and 27G), and the dependent variable measured was the alive cell fraction of the respective cell type. In case of statistically significant results post-hoc pairwise comparisons were meant to be conducted using Dunn's test with a Bonferroni correction to control for Type I error. Statistical significance was set at $p < 0.05$.

2.6 Chemicals and kits

Table 2.1: Chemicals

Chemical	Supplier
BioColl® Separation Solution	Bio&Sell, Germany
Dulbecco's phosphate buffered saline (PBS)	Biochrom GmbH, Germany
EDTA Solution pH 8.0 (0.5M)	AppliChem GmbH, Germany
Ethanol p.a.	SAV Liquid Production GmbH, Germany
Fetal Bovine Serum (FCS)	Gibco™, Thermo Fisher Scientific, USA

Penicillin-Streptomycin	Gibco™, Thermo Fisher Scientific, USA
Sodium azide	Carl Roth GmbH + Co. KG, Germany
Trypan Blue solution	Sigma-Aldrich, USA

Table 2.2: Kits

Kits	**Supplier**
AbC™ Total Antibody Compensation Bead Kit	Invitrogen™, Thermo Fisher Scientific, USA
LIVE/DEAD™ Fixable Near IR (780) Viability Kit	Invitrogen™, Thermo Fisher Scientific, USA

2.7 Buffers and media

Table 2.3: Buffers

Name	**Ingredients**
FACS buffer	500 ml PBS 10 ml FCS 2 ml EDTA = 2mM (0.5M stock solution) 1 ml sodium azide = 0.02% at 10% stock solution.

Table 2.4: Buffers

Medium	**Supplemented by**	**Supplier**
RPMI 1640 Medium, GlutaMAX™	- Penicillin/Streptomycin (1%) - FCS (10%)	Gibco™, Thermo Fisher Scientific, UK

2.8 Equipment and software

Table 2.5: Equipment

Equipment	Name	Supplier
Biological Safety Cabinets (BSC)	BioWizard Xtra Line Biosafety cabinet	Kojair Tech Oy, Finnland
Blood sampling cannula	Safety Multifly Cannula with Multiadapter	Sarstedt, Germany
Blood sampling monovettes	S-Monovette K3 EDTA 9 ml - red cap - (LxØ) 92 x 16 mm	Sarstedt, Germany
Cell Culture Flasks	Cellstar® Cell Culture Flasks 550ml, 175cm²	Greiner Bio-One GmbH, Germany
Cell culture tubes	Cellstar® Tube, 50ml, PP	Greiner Bio-One GmbH, USA
Centrifuge	Centrifuge 5810 R	Eppendorf, Germany
Closure Cones	B.Braun Combi-Stopper closure cones, Luer Lock	B.Braun, Germany
Disposable Pipettes	Corning® 5ml-50 mL Stripette™ Serological Pipettes	Corning, USA
Disposable syringes	B.Braun Omnifix® Luer Lock Solo disposable syringe, 5ml	B.Braun, Germany
Electronic Pipette	Eppendorf Xplorer® plus	Eppendorf, Germany
Hemocytometer	C-CHIP Disposable Hemocytometer Neubauer Improved	NanoEntek Inc., Korea

Incubator	Heracell™ 150i CO_2-Incubator	Thermo Fisher Scientific, USA
Multipipette	Eppendorf Multipette E3x	Eppendorf, Germany
Test tubes	Falcon® 5 ml Round Bottom Polystyrene Test Tube, 12x75mm	Corning, Mexico
Vitrectomy cutters (20G)	Disposable High Speed Vitrectors 20G / 8000 plus cpm, MID Labs	MIDlabs©, USA
Vitrectomy cutters (23G - 27G)	Disposable High Speed TDC Cutter 23G - 27 G / 8000 CPM DORC Continuum range	D.O.R.C.©, Netherlands
Vitrectomy machine	Qube™ pro vitrectomy system	Fritz Ruck Ophthalmologische Systeme GmbH, Germany
Vortex Mixer	PV-1 Vortex Mixer	Grant Instruments Ltd., UK

Table 2.6: Software

Software	**Developer**
BioRender	BioRender Inc., Canada
Excel	Microsoft Corporation, USA
FlowJo	FlowJo, LLC, USA
R: A language and environment for statistical computing	R Foundation for Statistical Computing, Vienna, Austria
Rstudio: Integrated Development Environment for R	PBC (Public Benefit Corporation), USA

Word	Microsoft Corporation, USA

2.9 Ethical approval and adherence to good scientific practice

The study was approved and registered (number 360/2024BO2) by the Ethics Committee of the University of Tübingen. All procedures were in accordance with the Declaration of Helsinki, German legislation, and the local ethics committee.

3 Results

In the period from April 2024 to December 2024 we conducted a total of six repetitions of the experimental workup shown above, of which three repetitions were made using lymphocytes isolated from peripheral blood samples and three repetitions made from *MYD88* positive lymphoma cells.

FACS analysis resulted in absolute cell counts and relative fractions, whereas absolute numbers had to be disregarded because of the nature of the investigational technique. One cannot assure with certainty which sample volume was analyzed, moreover one must set a defined bead count, which sets the limits for each count and makes them comparable. The respective fractions of cell populations can then reliably be used for further evaluation.

For each experimental setting we collected six datapoints for analysis. 36 datapoints could be collected from each experiment, resulting in 216 datapoints in total. Table 3-1 summarizes the results of our analysis.

Cell Type	Concentration (cells/mL)	Parameter	Kendall's τ (p-value)	Kruskal-Wallis χ^2 (p-value)
Healthy Lymphocytes	10^3	Gauge Size	0.1229 (0.3373)	1.4224 (0.7003)
		Cutting Rate	0.0230 (0.8618)	1.7432 (0.4183)
	10^4	Gauge Size	0.0289 (0.8214)	0.3694 (0.9465)
		Cutting Rate	-0.1150 (0.3841)	3.3168 (0.1904)
	10^6	Gauge Size	-0.0108 (0.9325)	0.2733 (0.965)
		Cutting Rate	-0.0843 (0.5233)	0.5466 (0.7609)
	Overall	Gauge Size	0.0243 (0.7377)	0.123 (0.9889)
		Cutting Rate	-0.0228 (0.7606)	0.1789 (0.9144)
MYD88-positive Lymphoma cells	10^3	Gauge Size	-0.1646 (0.1991)	1.8155 (0.6116)
		Cutting Rate	-0.2014 (0.1277)	2.4354 (0.2959)
	10^4	Gauge Size	-0.2602 (0.0422)	5.967 (0.1132)
		Cutting Rate	-0.0805 (0.5423)	0.5511 (0.7592)
	10^6	Gauge Size	-0.2731 (0.0331)	5.6849 (0.128)
		Cutting Rate	0.0096 (0.9422)	1.3429 (0.511)
	Overall	Gauge Size	-0.253 (0.00048)	13.337 (0.00396)
		Cutting Rate	-0.0485 (0.5165)	0.4505 (0.7983)

Table 3.1: Statistical Analysis of Gauge Size and Cutting Rate Effects on Lymphocyte and MYD88-Positive Lymphoma Cell Viability. The table summarizes the correlations between gauge size and cutting rate effects on MYD88-positive lymphoma cell and healthy lymphocyte viability at different cell concentrations. Notably,

a moderate negative correlation between gauge size and cell viability was observed at higher concentrations (1x10⁴cells/ml and 1x10⁶cells/ml cells/mL), with statistically significant Kendall's τ values.

3.1 Cell fractions of all samples taken together

3.1.1 Overall

The collected data exhibited a non-parametric distribution characterized by the presence of numerous outliers (see Figure 3-1). This was further supported by the Shapiro-Wilk test results, which indicated significant deviation from normality ($W = 0.93677$, $p < 0.0001$). Additional analysis after removal of outliers revealed no meaningful linear relationship among the variables.

Visual inspection of the scatter plots (see Figure 3-2) created from the summarized data seemed to show a decrease in alive cells with smaller gauge number and higher cutting rates. Even if only slightly, the calculated slopes seemed to support this notion as shown in Figure 3-3.

Statistical examination using correlation coefficients did indeed reveal this negative correlation, too. When evaluating this notion of a correlation further, it must be recognized that it can only be classified as very weak, if not statistically insignificant.

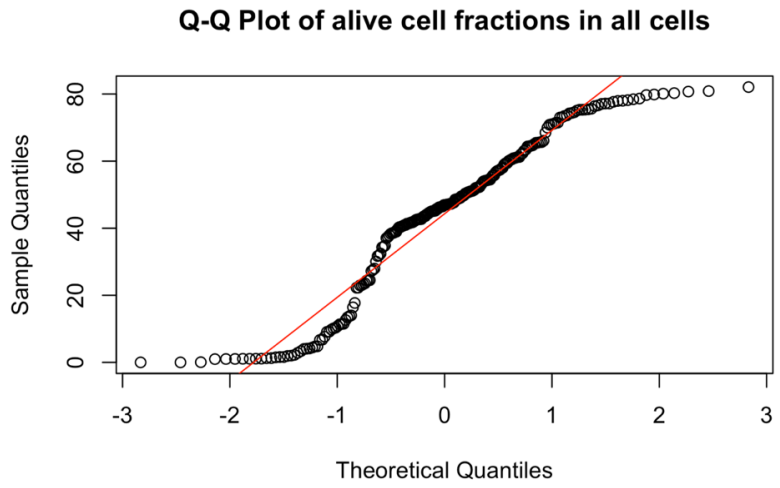

Figure 3-1: QQ Plot of alive cell fractions overall.

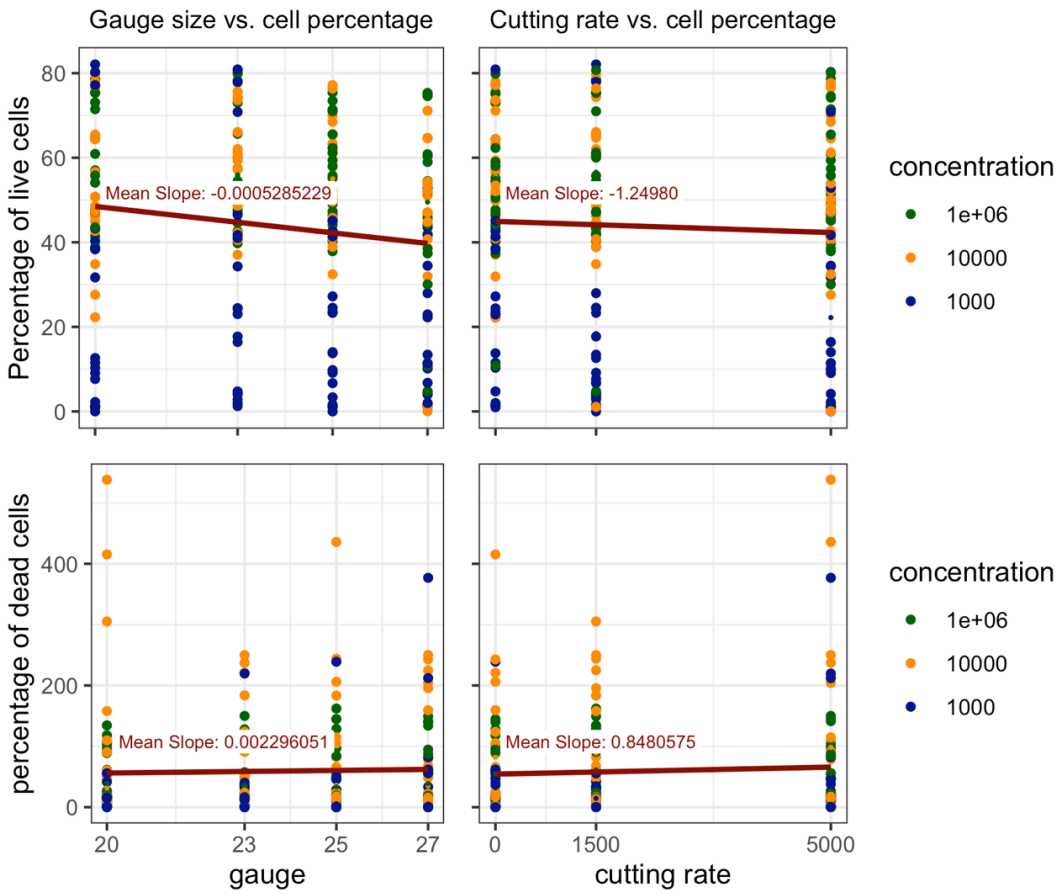

Figure 3-2: Scatterplots vitrectomy settings vs. cell fractions.

3.1.1.1 Gauge vs. live cell fractions

Correlation between selected gauge size and live cell fractions was evaluated by calculation of Kendall's Tau, resulting in r = -0.1116. This is to be interpreted as a weak negative correlation, meaning that a reduction in gauge size also led to a reduction in the proportion of living cells in the sample taken (also see boxplots in Figure 3-4). This correlation was statistically significant (p=0.028). Gauge size therefore is associated with changes in the living cell fractions in the overall dataset.

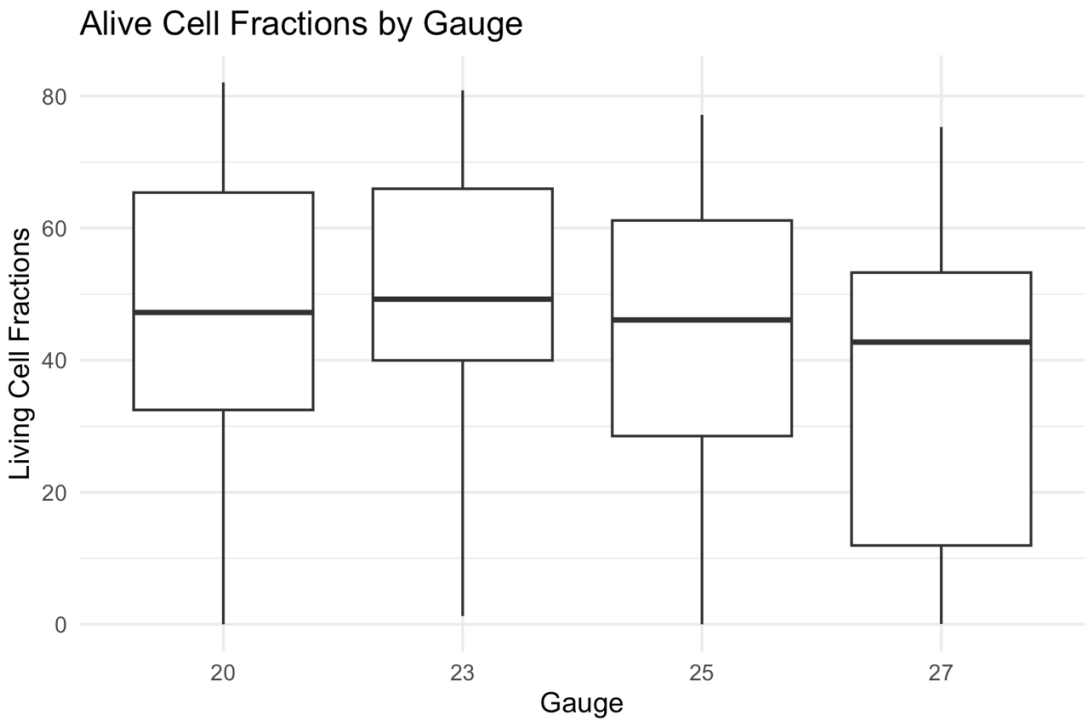

Figure 3-3: Boxplots Gauge vs. alive cells.

3.1.1.2 Cutting rate vs. live cell fractions

In order to assess the relationship between cutting rates and live cell fractions, a Kendall's Tau was calculated. The Kendall correlation coefficient was found to be r = -0.0386, indicating a very weak negative linear relationship between applied cutting rate and living cell fraction. The correlation was not statistically significant though (p= 0.46), In fact, changes in cutting rate are not associated with changes in living cell fractions in this dataset.

To further explore potential non-linear relationships the Kruskal-Wallis rank sum test was conducted to evaluate differences in the living cell fractions across the three groups defined by the applied cutting rate. The test showed no significant correlation (X^2 = 0.56901, df = 2, p-value = 0.7524), suggesting that the cutting rate does not have an impact on the relative number of alive cells. Visualization by boxplots undermines these results (see Figure 3-5).

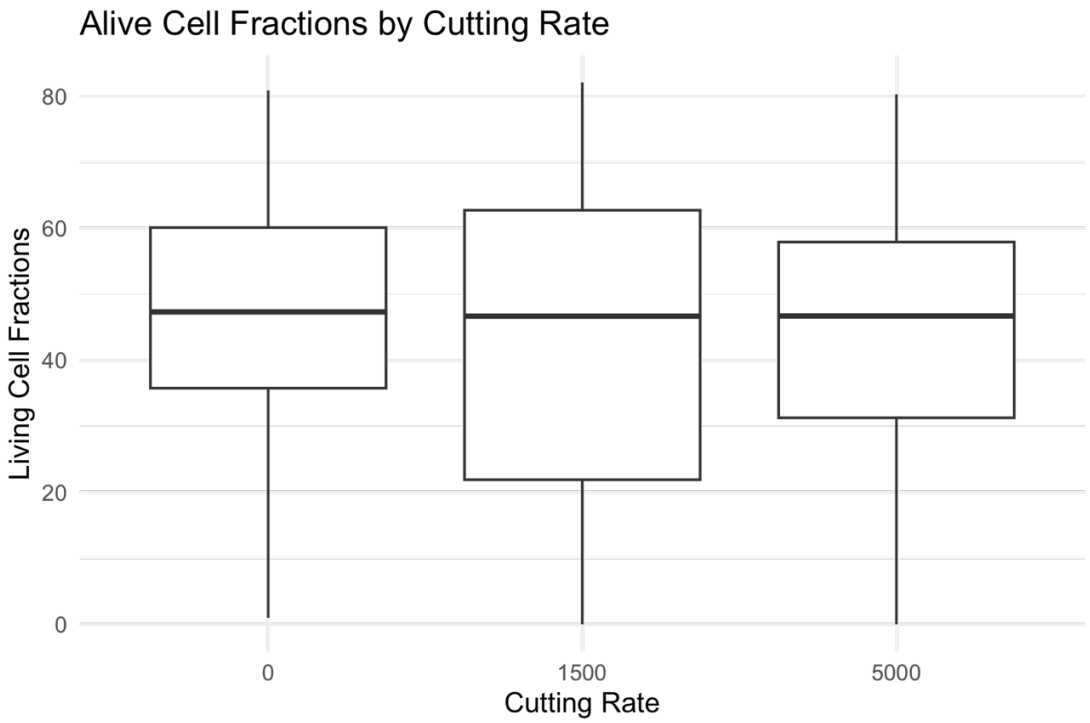

Figure 3-4: Boxplots Cutting rate vs. alive cells.

3.1.2 By each individual cell concentration

When the three sample concentrations were singled out, similar data distributions could be observed. Again, visual inspection of data distribution by QQ-plots suggested non-parametric distribution with several outliers. The Shapiro-Wilk normality test indicated significant deviations from normality for all three different cell concentrations (1x10³cells/ml, 1x10⁴cells/ml, and 1x10⁶cells/ml).

For cell concentration 1x10³cells/ml, the test resulted in W = 0.84431 ($p<0.01$), suggesting a strong deviation from normality. The cell concentration 1x10⁴cells/ml group showed a significant but less pronounced deviation from normality (W = 0.93995, p = <0.01). Similarly, cell concentration 1x10⁶cells/ml group also reflected a significant deviation from normality (W = 0.94404, p = <0.01). The consistently significant deviations from normal distribution indicate the necessity of non-parametric statistical approaches when analyzing cell fractions in each individual concentration alone (see Figure 3-6).

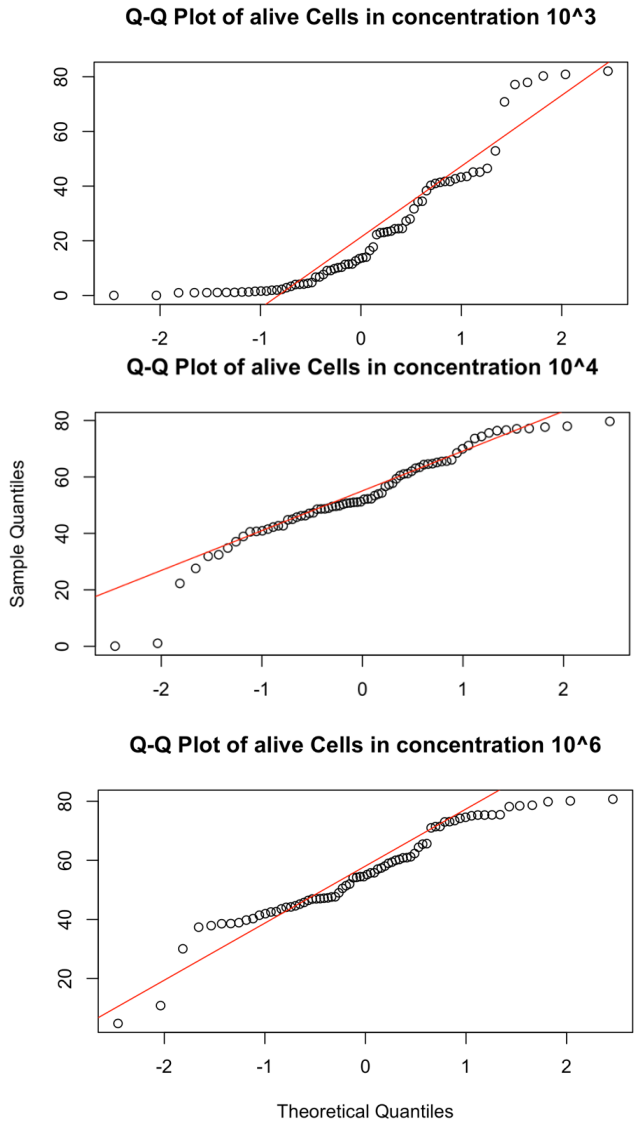

Figure 3-5: QQ-plots by concentration.

3.1.2.1 Concentration 1x10³cells/ml Analysis

At the lowest cell concentration (1x10³cells/ml), statistical evaluations demonstrated minimal correlational relationships. Cutting rate correlation yielded a weak negative Kendall's Tau of -0.0852 ($p = 0.3549$), while gauge size correlation showed an equally negligible coefficient of -0.0399 ($p = 0.6544$). Kruskal-Wallis tests confirmed no statistically significant differences across cutting rates ($\chi^2 = 2.0164$, $p = 0.3649$) or gauge sizes ($\chi^2 = 1.7061$, $p = 0.6356$).

3.1.2.2 Concentration 1x10⁴cells/ml Analysis

The intermediate cell concentration (1x10⁴cells/ml) exhibited similar patterns. Cutting rate correlation revealed a slightly more pronounced negative relationship ($\tau = -0.1028$, $p = 0.2643$), with gauge size showing a comparable weak negative correlation ($\tau = -0.0942$, $p = 0.2909$). Kruskal-Wallis analyses again demonstrated no statistically significant variations in cell viability differences across cutting rates ($\chi^2 = 1.4115$, $p = 0.4937$) or gauge sizes ($\chi^2 = 2.8179$, $p = 0.4206$).

3.1.2.3 Concentration 1x10⁶cells/ml Analysis

At the highest cell concentration (1x10⁶cells/ml), correlation patterns marginally diverged. Cutting rate correlation remained minimal ($\tau = -0.0181$, $p = 0.8443$), while gauge size correlation suggested a slightly more notable negative trend ($\tau = -0.1436$, $p = 0.1075$). However, these relationships remained statistically non-significant (for cutting rate $\chi^2 = 0.4589$, $p = 0.795$ and for gauge sizes ($\chi^2 = 3.775$, $p = 0.2868$).

3.1.2.4 Conclusion

The concentration-specific analysis confirmed the earlier findings that the vitrectomy settings marginally influence cellular viability in our experimental setup, however, these influences are not statistically significant. Figure 3-7 and figure 3-8 visualize these observations.

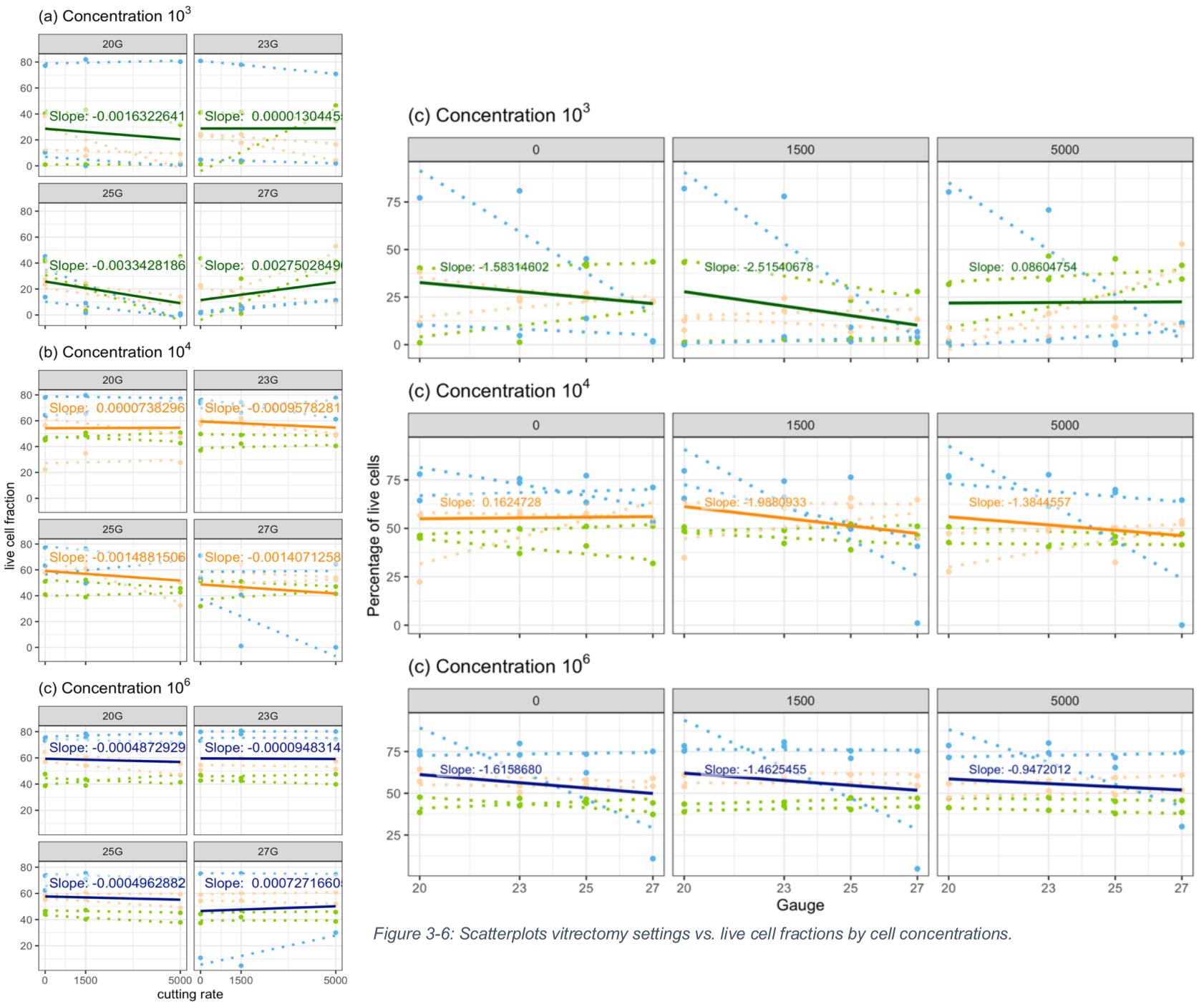

Figure 3-6: Scatterplots vitrectomy settings vs. live cell fractions by cell concentrations.

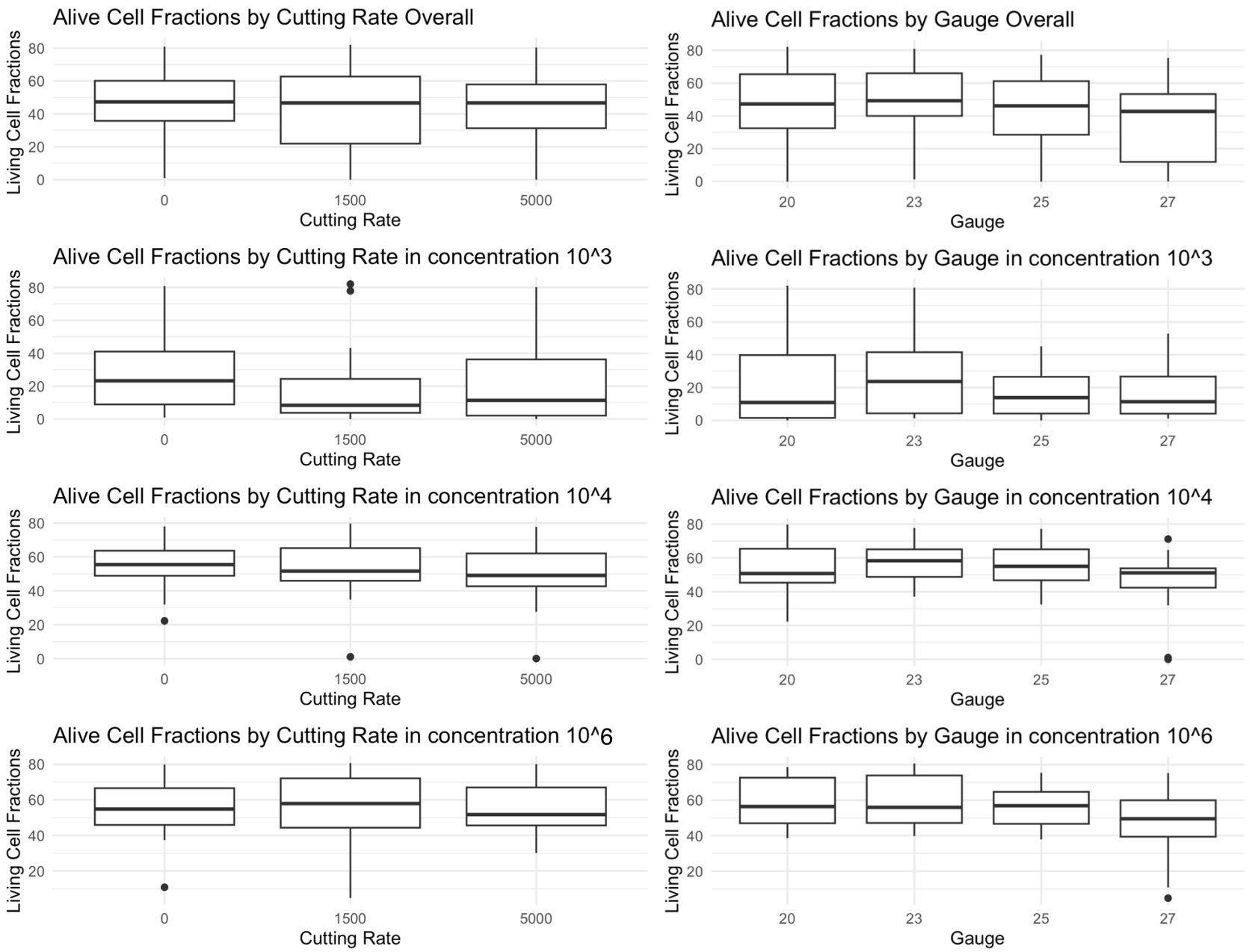

Figure 3-7: Box plots vitrectomy settings vs. life cell fractions by cell concentration and overall.

3.2 Lymphocytes and Peripheral Blood Mononuclear Cell (PBMC) Evaluation

Both lymphocyte and PBMC analyses revealed consistent patterns of statistical non-significance, suggesting that gauge size and cutting rate do not substantially influence viability of Lymphocytes in general and PBMCs in particular under our experimental conditions.

3.2.1 Lymphocyte Evaluation

The Shapiro-Wilk normality test for lymphocyte samples demonstrated significant deviations from a normal distribution across all experimental conditions (W= 0.8418, p-value<0.001). Figure 3.9 summarizes the viability trends of lymphocytes in comparison to gauge sizes and cutting rates used.

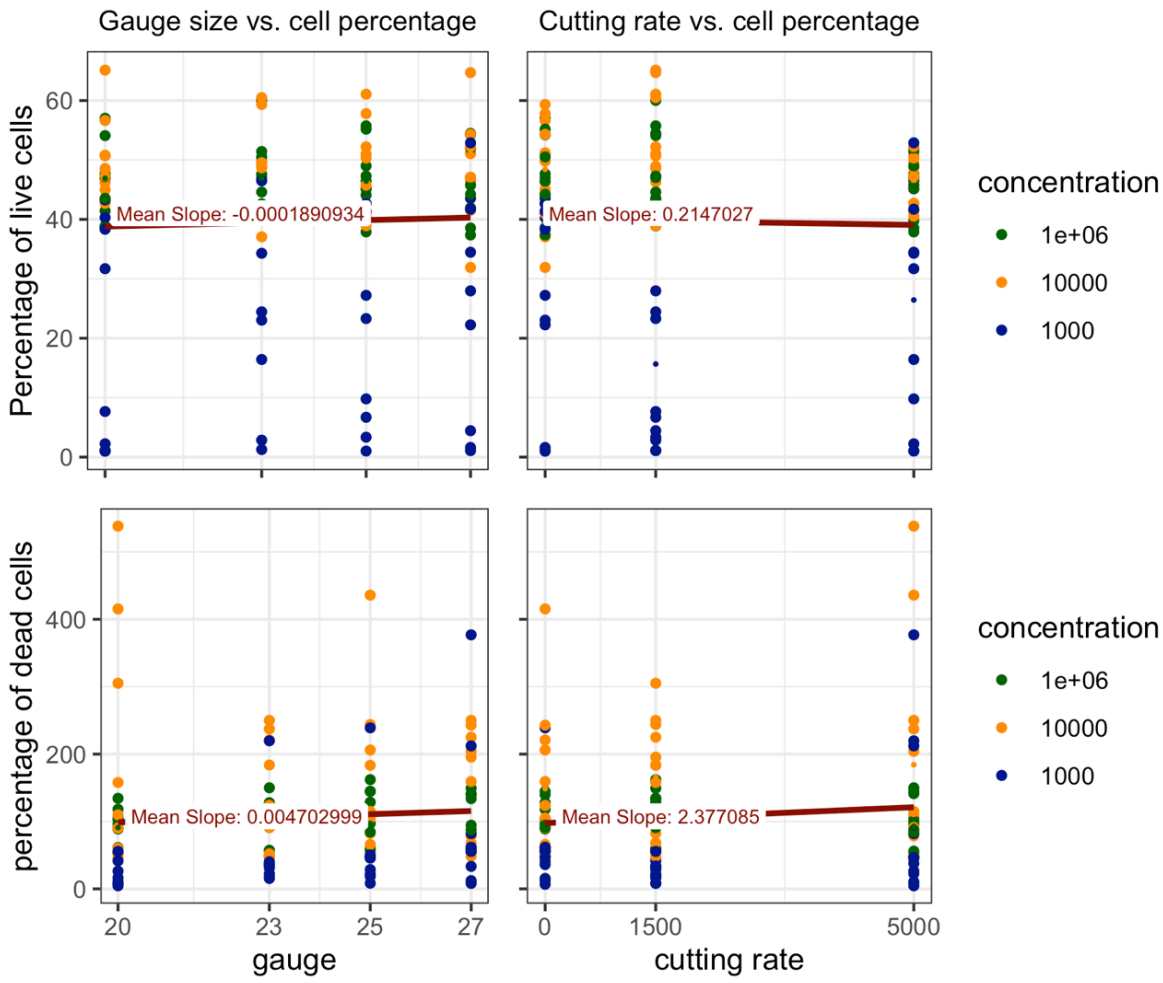

Figure 3-8: Lymphocyte survival - scatterplots showing vitrectomy settings vs. live and dead cell fractions.

3.2.1.1 Correlation of gauge size with cell viability

Gauge size correlations were inconclusive, with Kendall's Tau values ranging between -0.0108 and 0.1229. The associated p-values (consistently > 0.05) indicated no statistically significant association with lymphocyte survival rates (see Table 3.1 and Figure 3.10).

3.2.1.2 Correlation of cutting rate with cell viability

Cutting Rate Influence Kendall's Tau correlation analysis for cutting rates overall and singled out by individual concentrations yielded consistently weak negative correlations (τ ranging from -0.0228 to -0.1150). However, these correlations were statistically insignificant ($p > 0.05$), suggesting no meaningful relationship between cutting rates and lymphocyte viability (see Table 3.1 and Figure 3.10).

3.2.1.3 Statistical Verification

Statistical Verification Kruskal-Wallis rank sum tests consistently confirmed the lack of significant differences across cutting rates (χ^2 values: 0.1789 - 3.3168, $p > 0.05$) and gauge sizes (χ^2 values: 0.1231 - 1.4224, $p > 0.05$) in all concentrations taken together and singled out (see Table 3.1).

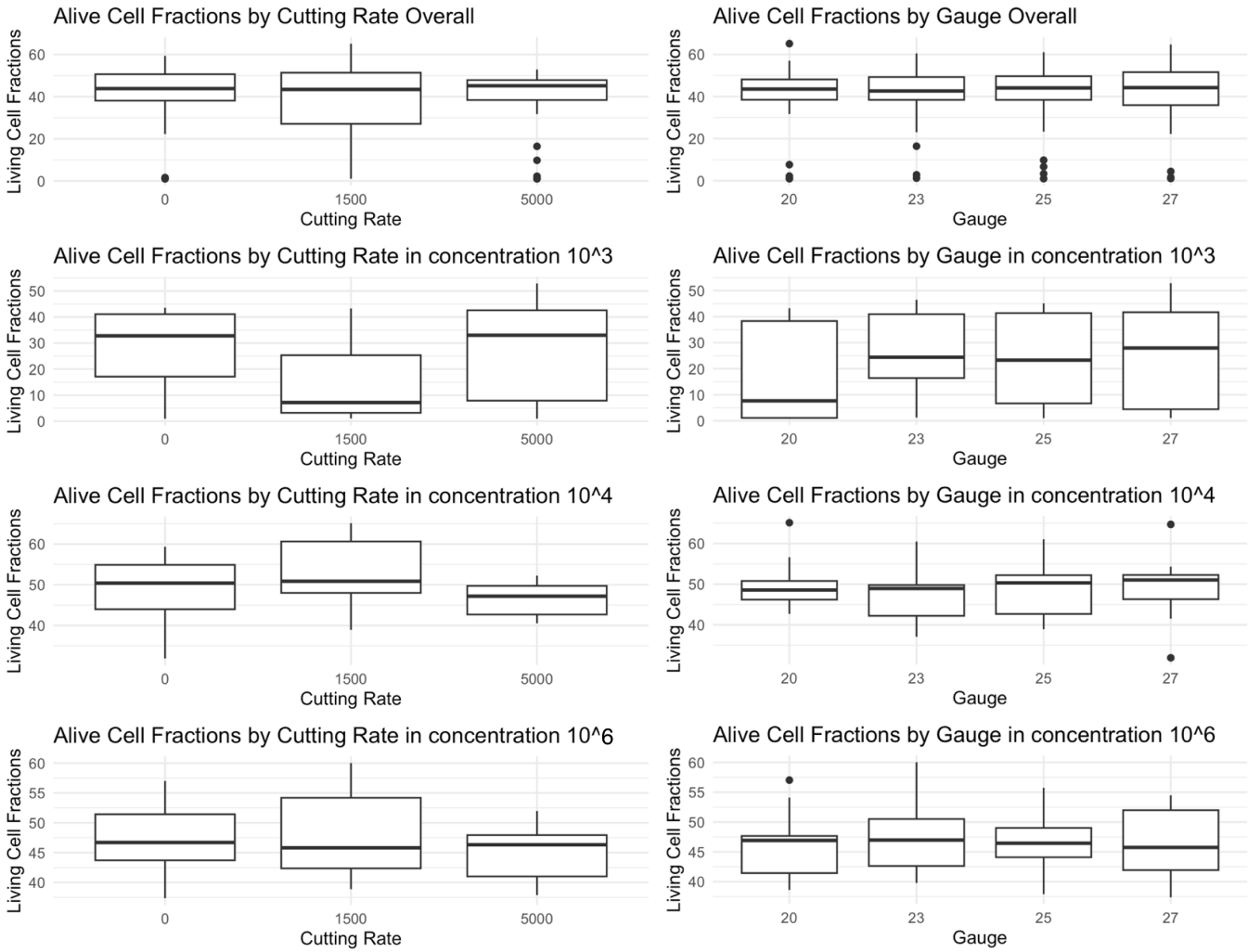

Figure 3-9: Lymphocytes - box plots vitrectomy settings vs. life cell fractions by cell concentration and overall.

3.2.2 Peripheral Blood Mononuclear Cells (PBMCs) Evaluation

Shapiro-Wilk tests for PBMC samples indicated non-normal distributions in overall measurements and the separate concentrations (W values ranging from 0.81333 to 0.98255), with p-values < 0.05, suggesting significant deviations from normality. Figure 3.11 summarizes the viability trends of PBMCs in comparison to gauge sizes and cutting rates used.

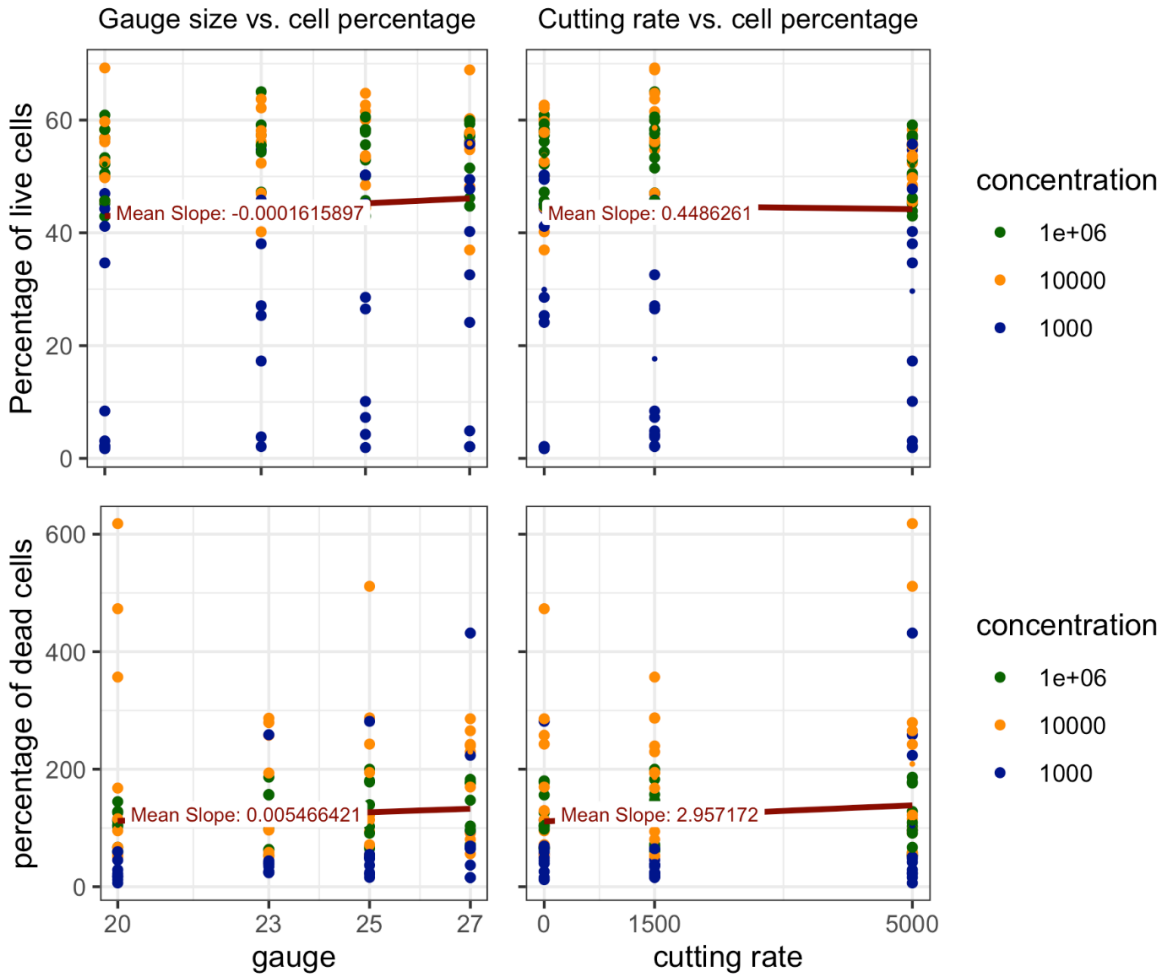

Figure 3-10: PBMCs - scatterplots of vitrectomy settings vs. cell fractions.

3.2.2.1 Correlation of gauge size with cell viability

Gauge size correlations were similarly weak and statistically insignificant, with Kendall's Tau values ranging from -0.0108 to 0.1301 ($p > 0.05$). (see Figure 3.12)

3.2.2.2 Correlation of cutting rate with cell viability

Cutting Rate Analysis Kendall's Tau correlation for cutting rates revealed weak negative correlations (τ between -0.0452 and -0.1610). These correlations were statistically non-significant ($p > 0.05$), indicating no substantial impact on PBMC viability. (see Figure 3.12)

3.2.2.3 Statistical Verification

Kruskal-Wallis tests consistently demonstrated no statistically significant differences across cutting rates (χ^2 values: 0.9185 - 5.4099, $p > 0.05$) or gauge sizes (χ^2 values: 0.1732 - 1.1381, $p > 0.05$).

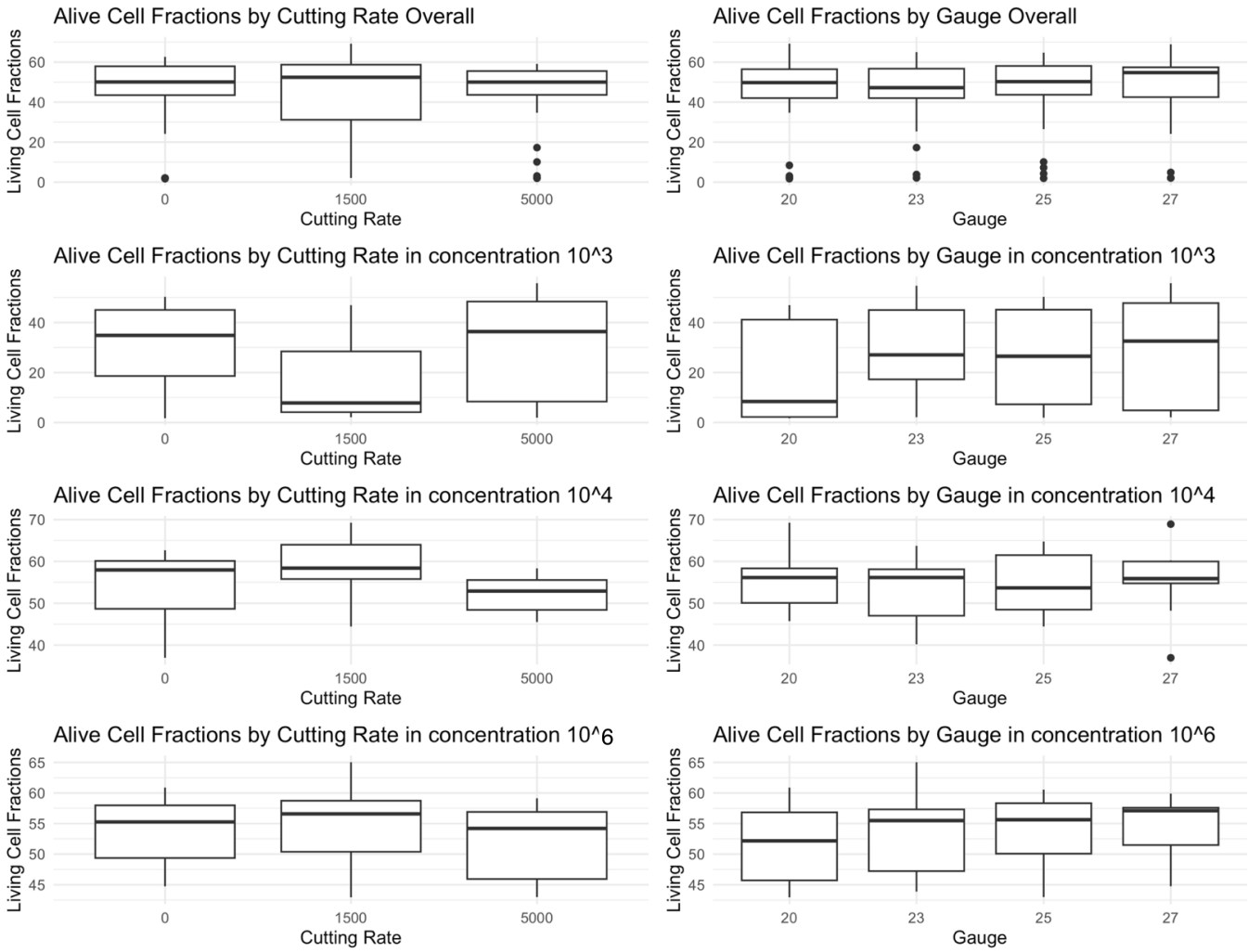

Figure 3-11: PBMCs - box plots of vitrectomy settings vs. life cell fractions by cell concentration and overall.

3.3 *MYD88*-positive lymphoma cell Evaluation

Shapiro-Wilk normality tests for *MYD88*-positive lymphoma cell samples consistently revealed significant departures from normal distribution (W values ranging from 0.71125 to 0.85798, p-values < 0.05), indicating non-parametric data characteristics. Figure 3.13 summarizes the viability trends of *MYD88*-positive lymphoma cells in comparison to gauge sizes and cutting rates used.

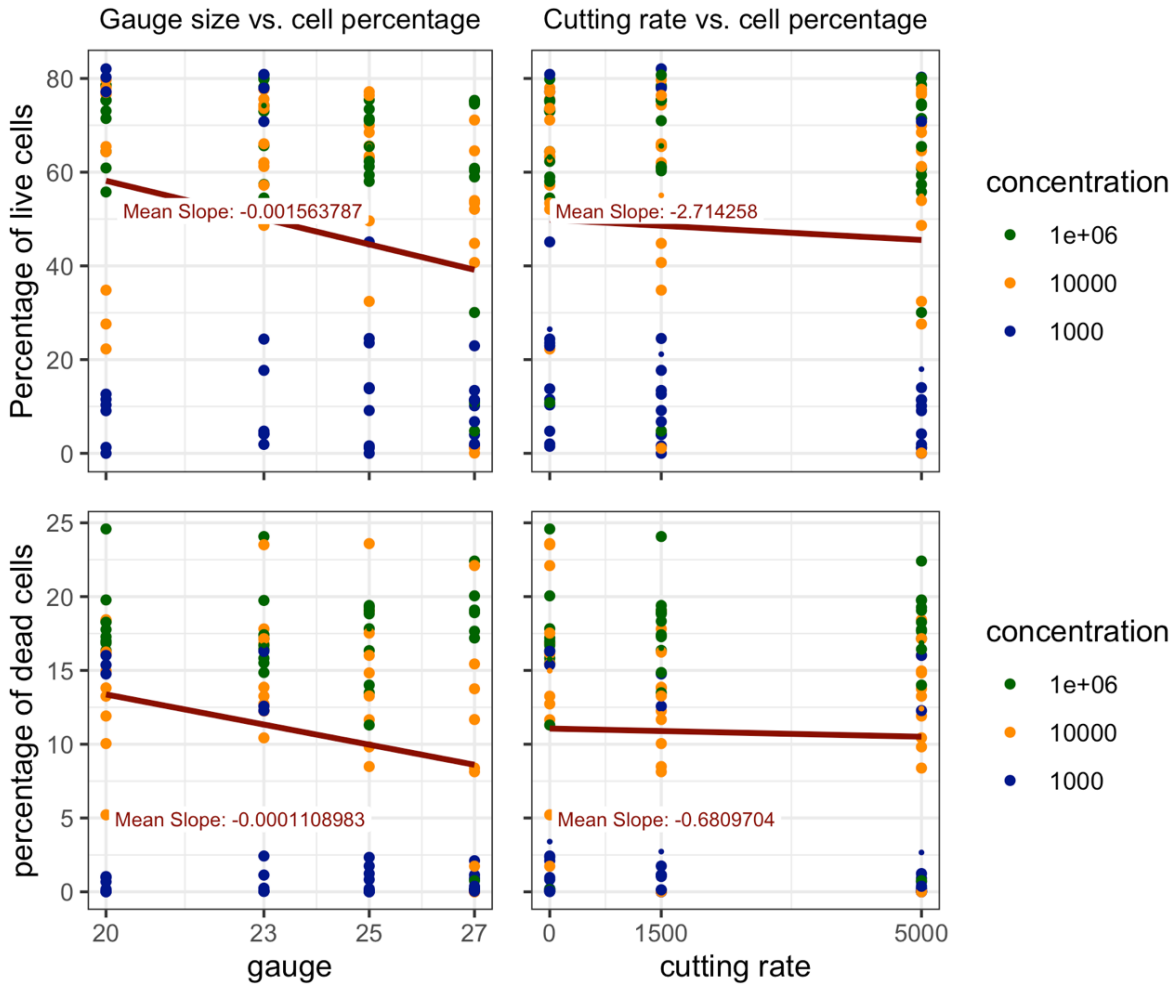

Figure 3-12: MYD88 positive lymphoma cell - scatterplots of vitrectomy settings vs. cell fractions.

3.3.1 Correlation of gauge size with cell viability

Notably, gauge size correlations revealed more interesting patterns. Overall analysis showed a statistically significant negative correlation ($\tau = -0.253$, $p < 0.01$), indicating a potential inverse correlation between gauge size and cell

viability. This trend was evident with correlation coefficients ranging from -0.164 to -0.273 (see Table 3.1 and Figure 3.14).

3.3.2 Correlation of cutting rate with cell viability

Kendall's Tau correlation analysis for cutting rates demonstrated weak and statistically non-significant correlations across different experimental conditions. Correlation coefficients ranged from -0.0485 to 0.0096, with p-values consistently > 0.05, suggesting no correlation between cutting rates and cell viability (Table 3.1 and Figure 3.14).

3.3.3 Statistical verification

Kruskal-Wallis rank sum tests for cutting rates consistently demonstrated no statistically significant differences (χ^2 values: 0.4506 - 2.4354, $p > 0.05$), reinforcing the lack of impact on cell viability.

Kruskal-Wallis tests for gauge sizes showed mixed results. The overall analysis revealed a statistically significant difference ($\chi^2 = 13.337$, $p < 0.01$), suggesting a potential influence of gauge size on cell viability. However, individual experimental conditions showed less pronounced effects (χ^2 values: 1.8155 - 5.967, with some p-values approaching but not reaching statistical significance).

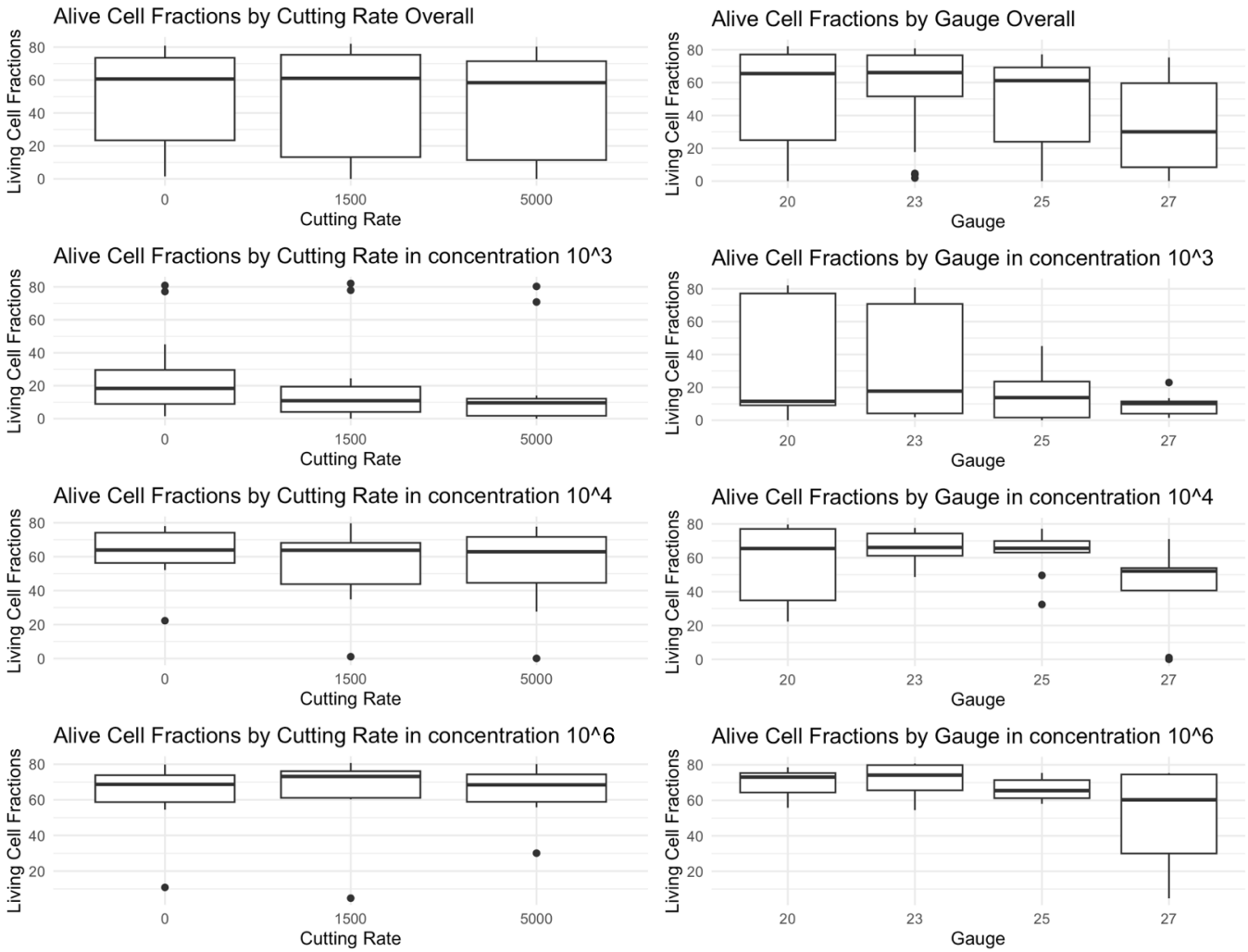

Figure 3-13: MYD88-positive lymphoma cells - box plots of vitrectomy settings vs. life cell fractions by cell concentration and overall

4 Discussion

This work addressed the persistent challenge for clinicians in diagnosing vitreoretinal lymphoma (VRL) by investigating and refining vitreous sampling techniques by vitrectomy. Recognizing the critical need for optimized methods, particularly given the diagnostic difficulties and potential for delayed treatment in VRL, this research evaluated the impact of gauge size and cutting rate on the survival of lymphocytes, comparing the effects on healthy lymphocytes and malignant lymphoma cells.

4.1 Key findings and interpretation

Our findings indicate that, in healthy lymphocytes overall, but also in PBMCs alone, variations in gauge size and cutting rate during vitrectomy had no significant impact on cell survival across different dilutions. However, a notable difference was measurable when examining malignant lymphoma cells. Larger gauge lumina demonstrated a significantly higher cell survival rate across all concentrations tested, while variations in cutting rates had no effect. These results suggest that lymphoma cells are more sensitive to the mechanical forces exerted during vitrectomy with smaller gauge instruments, highlighting the importance of instrument selection during VRL diagnosis. In fact smaller gauge sizes may be associated with reduced cell viability in *MYD88*-positive lymphoma cells, warranting further investigation.

This study included healthy lymphocytes and indicated no impact of different settings in vitrectomy on these healthy cells. However, malignant cells seem to exhibit different properties compared to healthy cells. Malignant cells are less abundant in the vitreous and more fragile, particularly if the patient has received corticosteroids before the intervention, making the establishment of a diagnosis more difficult (Dawson et al., 2018). Our results also suggested increased cellular sensitivity in these pathologically altered cells. The structural integrity and viability of lymphoma cells may be more susceptible to mechanical manipulation compared to healthy peripheral blood-derived cell populations. The differential

response between healthy lymphocytes and lymphoma cells underscores the potential fragility of malignant cells and highlights the importance of carefully optimizing surgical biopsy protocols when working with potentially unstable cellular systems, such as vitreoretinal lymphoma cells.

This increased sensitivity of lymphoma cells to mechanical stress during vitrectomy may contribute to the challenges in obtaining adequate diagnostic samples, potentially explaining the need for repeated diagnostic procedures in some cases.

4.2 Comparison with previous studies

Several studies have been established for vitreous biopsy in lymphoma case.

Kanavi et al. contrasted 25G lymphoma biopsies to literature results of 20G and found superiority for 25G biopsy. However, the most recent included study on PIOL diagnostic yield in 20G was from 2008 and showed data of a 15-year review (1990-2005) on cytopathological findings for PIOL (Wittenberg et al., 2008). The better results for 25G might also be linked to improved general vitrectomy settings and technologies.

Tekumalla et al. found that the cutting rate of 25 G vitrectomy did not affect lymphoma cell viability. They even used rates up to 15,000 cpm. These findings are in line with our study. Contrary, an older study with 20 G recommended only cutting rates up to 1000 cpm for vitreous biopsy in lymphoma suspects (Dalal et al., 2014; Jiang et al., 2014). These results are probably also linked to older cutter designs and less stable flow dynamics in older machines. The duty cycle and the design of the cutter may have influenced the results; however, this aspect has not been investigated in our study. Nevertheless, a study by Ulltang et al. indicated that TDC probes demonstrated superior performance in acquiring cytohistological probe quality of solid liver tissue (Ulltang et al., 2021).

For bacterial endophthalmitis and diagnostic vitrectomy a prospective laboratory in vitro experiment was established by Almeida et al. (Almeida et al., 2016). The study was performed with 20-, 23- and 25-gauge vitrectors at cutting rate of zero,

1500 and 5.000 cpm. This protocol was adopted and expanded by employing 27G cutters for our experiment. Viable bacterial colonies were established for all gauge instruments, cutting speed and aspiration rates without any statistical difference. The most potent culture growth was recognized in 20-gauge vitrectomy set at 1500 cpm and 25-gauge vitrectomy with 5000 cpm (Almeida et al., 2016). The characteristics of a bacterial sample cannot be completely applied to a vitreous sample in the context of lymphoma diagnosis.

Our study improves upon previous works by Jiang et al. and Tekumalla et al., which relied on conventional hemacytometer counting (Jiang et al., 2014; Tekumalla et al., 2023), by employing Fluorescence-Activated Cell Sorting (FACS). FACS offers rapid, multiparametric analysis of thousands of cells per second, eliminating operator subjectivity, and enabling cell sorting based on specific characteristics (Cossarizza et al., 2017). While FACS may exhibit lower accuracy in routine cell density measurements compared to counting chambers, its high-throughput capabilities and ability to analyze multiple cellular parameters simultaneously make it superior for comprehensive cell analysis and characterization in this context.

4.3 Cutting Rate and Cell Viability

Not only the gauge diameter has a paramount share in vitrectomy but cutter designs and cutting rates. Modern systems allow cutting rates up to 20.000 cpm or more. With 5.000 cpm in this study the established settings here were already quite high and probably higher than normally used in vitreous sampling. The finding that cutting rate did not significantly affect cell survival, even at the relatively high rate of 5,000 cpm used in this study, is consistent with some previous research (Tekumalla et al., 2023). However, it contradicts earlier studies that recommended lower cutting rates for vitreous biopsy in lymphoma suspects (Dalal et al., 2014). This discrepancy may be attributed to advancements in cutter designs and flow dynamics in modern vitrectomy systems. The bi-blade, two-dimensional cutting (TDC) vitrectomes used in this study, which offer near-100%

duty cycles and reduced turbulence, may mitigate the negative impact of high cutting rates on cell survival [Mariotti et al., 2016; Mitsui et al., 2016; Pandit et al., 2023]. These double-sided blades cut both in the forward and backward direction, allowing for higher efficiency and a constant aspiration regardless of cutting speed. This design reduces turbulences and shortens the time needed for core vitrectomy, potentially contributing to better cell preservation.

4.4 Evolution of Vitrectomy Techniques

Since Machemer developed the first 17G vitrectomy in the 1970s, vitrectomy systems have undergone significant evolution. Newer systems have introduced more stable flows and dynamics (de Oliveira et al., 2016). When deciding on the appropriate lumen diameter, surgeons must balance several factors, including the durability and flexibility of the instruments, the pace of vitreous removal, and wound management considerations.

The development of microincision vitrectomy surgery (MIVS) has allowed for smaller incisions, potentially reducing surgical trauma and improving postoperative recovery. While larger gauge diameters allow for more rapid vitreous removal, they also carry increased risks of wound leakage, hypotony, and infection (Pandit et al., 2023). Our experiment demonstrated that using smaller gauge diameters results in increased strain: the resistance in the sampling tube is higher, and the sampling process took longer compared to using conventional 20G or 23G vitrectomy instruments. These findings align with results from several studies, particularly those focusing on newer 27G techniques (Pandit et al., 2023).

Innovations in cutter design, such as the development of dual-port cutters and increased cut rates (up to 20,000 cpm in some systems), have improved the efficiency of vitreous removal while potentially reducing traction on the retina. These advancements may contribute to more efficient and safer diagnostic biopsies.

Adaptive fluidics systems in modern vitrectomy machines aim to maintain consistent intraocular pressure throughout the procedure, potentially reducing the risk of hypotony and its associated complications. This could be particularly beneficial in diagnostic procedures where maintaining a stable ocular environment is crucial for preserving cellular integrity.

4.5 Dynamics in Vitrectomy

The vitreous is based on liquid fractions and solid fragments (Sebag, 2016). Therefore, physics of both fluid material and solid matter apply when regarding forces exerted on the vitreous body in vitrectomy (Magalhaes et al., 2011).

The impact of gauge size on cell survival can be explained by fluid dynamics principles. Liquids are subject to the Hagen-Poiseuille equation that states a relative increase of resistance of flow and increase of velocity depending on the lumen diameter. Accordingly, as the diameter of the sampling tube decreases in smaller gauge sizes, the resistance to flow increases dramatically (to the fourth power of the radius). This increased resistance may lead to greater shear stress on cells passing through the instrument, particularly affecting the more fragile lymphoma cells.

This principle has a particularly significant effect when comparing 27G vitrectomy to larger gauges such as 23G (0.4 mm vs. 0.64 mm lumen diameter) and might be considered when deciding for the right sampling instrumentation. The substantial increase in flow resistance with smaller gauges may contribute to the observed higher survival rate of lymphoma cells with larger gauge instruments. This finding suggests that the choice of gauge size is not merely a matter of surgical convenience but can have direct implications for the quality and quantity of diagnostic material obtained.

For solid vitreous fragments displacement and deformation forces play a role (Magalhaes et al., 2011). Newton's second law states that the displacement force of a solid is proportional to mass and acceleration ($F = ma$) (Fox & McDonald, 1995). When increasing the cutting rate, the amount of vitreous and therefore

solid particles pulled into the cutter decreases. The cut particles of vitreous become smaller and are being pulled continuously into the cutter lumen on the basis of decreased deformation forces (Magalhaes et al., 2008). Decreased duty cycles can also reduce the size of vitreous fragments. How these properties do have influence on the sampling in vitreous sampling needs to be investigated further.

4.6 Challenges and Limitations of vitrectomy

Despite its advantages, PPV is not without limitations. Challenges such as low biopsy volume, fragile lymphoma cells, and hypocellular specimens frequently necessitate repeat procedures or even retinal biopsies, delaying diagnosis by weeks to months (Cassoux et al., 2000; Fadlelseed et al., 2024; Soussain et al., 2021). Such delays are clinically consequential, as early intervention improves both ocular and systemic outcomes in VRL (Chan & Sen, 2013).

These hurdles highlight the urgent need for standardized protocols for vitreous biopsy processing, including rapid fixation, optimized cytocentrifugation, and integration of molecular techniques like *MYD88* mutation analysis to enhance diagnostic yield (Chan et al., 2011; Menean et al., 2023). A synergistic approach combining PPV with advanced molecular methods may bridge current diagnostic gaps. For example, next-generation sequencing of vitreous-derived DNA can detect clonal lymphoid populations even in paucicellular samples, potentially reducing reliance on repeat surgeries (Menean et al., 2023). Additionally, standardizing biopsy handling across institutions could mitigate variability in diagnostic accuracy (Chan et al., 2011).

Our study contributes to this effort by providing insights into the optimal gauge size for preserving lymphoma cell viability during vitrectomy. Our findings shed light on one potential factor contributing to the challenge of obtaining adequate biopsy samples: the increased fragility of lymphoma cells compared to healthy lymphocytes during vitrectomy. The observed higher survival rate of lymphoma cells with larger gauge instruments suggests that smaller gauge instruments may

inflict greater mechanical stress on these fragile cells, potentially leading to cell lysis and reduced diagnostic yield.

4.7 Liquid Biopsies in context with vitrectomy

While liquid biopsies represent an exciting frontier in cancer diagnostics, they currently lack the sensitivity and specificity required to supplant PPV and direct cytological analysis in VRL diagnosis due to its ability to obtain high-quality vitreous samples with superior cellularity, which reduces false-negative rates and allows for comprehensive multimodal analyses, including cytology, flow cytometry, and molecular profiling (Carbonell et al., 2021; Coupland, 2012; Kwak et al., 2023). Cell-free DNA (cfDNA) analysis of intraocular fluid, for instance, has demonstrated a 5% false-positive rate due to nonspecific inflammatory signals, limiting its utility as a standalone diagnostic tool (Bonzheim et al., 2023). Studies consistently highlight that PPV yields specimens with superior cellularity compared to aqueous humor aspiration or liquid biopsies, significantly reducing false-negative rates (Coupland, 2012; Kwak et al., 2023).

The low cellular yield of liquid biopsies precludes comprehensive immunophenotyping, a cornerstone of lymphoma subtyping (Sobolewska et al., 2021). While cfDNA sequencing may serve as an adjunct for monitoring relapse or residual disease, its diagnostic shortcomings in primary VRL underscore the enduring need for PPV and direct cytopathological analysis (Huang et al., 2024). The diagnostic accuracy afforded by PPV is further enhanced by its capacity to support multimodal analyses, including cytology, flow cytometry, and molecular profiling (Carbonell et al., 2021).

The limitations of liquid biopsies in VRL diagnosis are particularly evident when considering the need for accurate disease classification. VRL encompasses a spectrum of lymphoid malignancies, each with distinct molecular profiles and treatment requirements. The comprehensive cellular analysis attained by PPV-obtained samples allows for precise classification, which is crucial for tailoring treatment strategies and predicting outcomes. Efforts must therefore focus on refining PPV-derived analyses, establishing standardized protocols, and

integrating novel technologies to expedite diagnosis and improve patient outcomes.

4.8 Limitations of the Study

Our study has several limitations that should be considered when interpreting the results. While Flow Cytometry (FACS) offers rapid, multiparametric analysis and eliminates operator subjectivity, its accuracy in routine cell density measurements may be lower compared to traditional counting chambers (Camacho-Fernández et al., 2018; Cossarizza et al., 2017; McKinnon, 2018). However, its high-throughput capabilities and ability to analyze multiple cellular parameters simultaneously make it superior for comprehensive cell analysis in this context. The use of healthy lymphocytes as a control, while providing a baseline for comparison, may not fully replicate the properties of lymphoma cells in vivo, particularly in patients who have received prior treatments such as corticosteroids (Dawson et al., 2018).

Additionally, while gauge size and cutting rate were investigated, other factors such as aspiration pressure and infusion rate were not systematically evaluated. These parameters could potentially influence cell survival and sample quality. However, it is important to note that in vivo diagnostic vitrectomy procedures often involve manual aspiration using a syringe without a defined aspiration pressure, and are typically performed under air infusion or with the infusion turned off (Hwang et al., 2014; Malinowski, 2010). Our experimental model mirrors this in-vivo approach closely, enhancing its clinical relevance and comparability to real-world diagnostic procedures.

Furthermore, studies have shown that undiluted vitreous samples are typically obtained with the infusion off to prevent dilution of the specimen, which aligns with our experimental setup (Hwang et al., 2014). This technique allows for the collection of approximately 1.5–2 mL of undiluted vitreous fluid, providing a sufficient sample for cytopathology, flow cytometry, and other diagnostic tests (Hwang et al., 2014; Menean et al., 2023). The similarity between our model and

clinical practice in these aspects strengthens the validity of our findings and their applicability to diagnostic vitrectomy procedures for intraocular lymphoma.

Some outliers, potentially attributable to procedural errors in tube allocation, were identified. Additional repetitions and a larger number of data points are necessary to obtain more conclusive results. More extensive studies with larger sample sizes and additional replicates are needed to draw definitive conclusions about any conclusive relationships. It is important to note that the overall cell density in this experiment was likely artificially higher than in real-world settings. In lymphoma patients, malignant cells are probably dramatically lower in proportion, with healthy lymphocytes dominating the sample.

The properties of the human vitreous body might influence cell behavior and viability in ways not captured by this in vitro model. Results from this study cannot be fully transferred to the in vivo setting without further validation. Future studies could benefit from using primary lymphoma cells obtained from patient samples, although this approach presents significant ethical and practical challenges. These limitations underscore the need for cautious interpretation of our results and highlight areas for future research to enhance our understanding of lymphoma cell behavior in the context of vitreoretinal procedures. Despite these constraints, we provide valuable preliminary data and a foundation for further investigations in developing evidence-based guidelines for VRL sampling.

4.9 Implications for Clinical Practice

Our findings have important implications for clinical practice in VRL diagnosis. When performing vitreous biopsies for suspected VRL, surgeons should carefully consider the gauge size of the vitrectomy instrument. Based on our results, larger gauge instruments may be preferable to minimize mechanical stress on fragile lymphoma cells and improve diagnostic yield. Further research is needed to validate these findings in vivo and to determine the optimal gauge size and vitrectomy settings for VRL diagnosis.

However, the choice of gauge size should be balanced against other clinical considerations, such as the need for minimally invasive surgery and rapid postoperative recovery. The development of advanced 27G systems with improved fluidics and cutting efficiency may help bridge the gap between the desire for smaller incisions and the need for optimal sample collection.

An improvement of the right technique for diagnostic vitrectomies with suspicion for VRL can prevent multiple tissue biopsies and thus enhance effectiveness and reduce costs and burden for patients and physicians and establish a diagnosis earlier.

4.10 Broader Implications for Ocular Oncology

The findings of this study have implications beyond VRL diagnosis. The principles of optimizing vitreous sampling for cell preservation could be applied to other intraocular malignancies where cytological diagnosis is crucial, such as uveal melanoma or metastatic tumors to the eye. Furthermore, the insights gained regarding the fragility of malignant cells during vitrectomy could inform the development of gentler tissue acquisition techniques for a range of ophthalmic pathologies.

4.11 Future Directions and Emerging Technologies

A synergistic approach combining PPV with advanced molecular methods may bridge current diagnostic gaps. For example, next-generation sequencing of vitreous-derived DNA can detect clonal lymphoid populations even in paucicellular samples, potentially reducing reliance on repeat surgeries (Menean et al., 2023). Additionally, standardizing biopsy handling across institutions could mitigate variability in diagnostic accuracy (Chan et al., 2011).

Emerging technologies such as single-cell RNA sequencing and proteomics may further enhance the diagnostic capabilities of vitreous samples obtained through PPV. These techniques could provide unprecedented insights into the molecular

heterogeneity of VRL, potentially identifying new diagnostic markers and therapeutic targets.

The integration of artificial intelligence and machine learning algorithms in the analysis of vitreous samples represents another promising frontier. These technologies could potentially improve the sensitivity and specificity of VRL diagnosis by identifying subtle patterns in cytological and molecular data that may be missed by human observers.

4.12 Conclusion

In conclusion, this study contributes to a better understanding of the factors influencing cell survival during vitreous sampling for VRL diagnosis. Our findings suggest that larger gauge instruments may improve the survival of fragile lymphoma cells, potentially enhancing diagnostic yield. The lack of significant impact from cutting rates, even at high speeds, supports the use of modern high-speed cutters in diagnostic vitrectomy.

While liquid biopsies represent an exciting frontier in VRL diagnosis, PPV remains the gold standard due to its currently unparalleled diagnostic and therapeutic utility. Efforts must therefore focus on refining PPV-derived analyses, establishing standardized protocols, and integrating novel technologies to expedite diagnosis and improve patient outcomes.

By optimizing vitrectomy techniques and integrating advanced molecular methods, we can improve the accuracy and timeliness of VRL diagnosis, leading to better outcomes for patients with this challenging condition. As we continue to refine our diagnostic approaches, the integration of novel technologies and standardized protocols will be crucial in advancing our ability to diagnose and manage VRL effectively.

The field of vitreoretinal surgery is constantly evolving, with advancements in MIVS equipment and better visualization techniques making once daunting procedures more commonplace. These improvements have resulted in shorter

surgery times, smaller incisions, and higher levels of surgical safety, ultimately leading to improved patient outcomes. As technology continues to progress, we can expect even more innovations in vitrectomy surgery that will further enhance the quality of life and outcomes for patients with VRL and other vitreoretinal pathologies.

Further research should focus on validating our findings in clinical settings, exploring the impact of other vitrectomy parameters on sample quality, and investigating the potential of emerging technologies to further enhance VRL diagnosis and management. Additionally, studies using primary lymphoma cells obtained from patient samples could provide more accurate insights into the behavior of VRL cells during vitrectomy, providing practical guidance to clinicians, enabling evidence-based decision making, and ultimately improving the care of lymphoma patients.

5 Summary

Purpose: To assess whether vitrectome size and cutting rate have an impact on cell survival of healthy lymphocytes and lymphoma cells during diagnostic vitrectomy in an in vitro model.

Methods: In the first experiment, healthy lymphocytes were isolated from blood samples of one healthy individual. In the second experiment, cultivated *MYD88* positive lymphoma cells derived from a commercially available cell line were used. Suspensions with defined cell concentrations ($1x10^3$ cells/ml, $1x10^4$ cells/ml and $1x10^6$ cells/ml) were subjected to vitrectomy under controlled conditions, using aspiration only or varying cutting rates of 1500/min and 5000/min with vitrectome sizes of 20G, 23G, 25G and 27G. Three technical replicates were performed for each condition. Cell integrity in post-vitrectomy samples was assessed via fluorescence activated cell sorting (FACS). To verify statistically significant differences between groups, the Kruskal-Wallis test was employed.

Results: No correlation was observed between lymphocyte survival and either gauge size or lower cutting rates in healthy lymphocytes. However, a significant correlation between vitrectome size and cell survival was observed for lymphoma cells (Kendall's tau $\tau = -0.253$, $p = 0.00048$, Kruskal-Wallis $\chi^2 = 13.337$, $p = 0.00396$).

Conclusions: In our study, larger vitrectome lumen diameters were associated with higher survival rates of lymphoma cells, suggesting that a careful approach during vitrectomy may enhance diagnostic yield.

Keywords: Vitrectomy, gauge, cutting rate, vitreoretinal lymphoma, vitreous biopsy, lymphocyte, lymphocyte survival, FACS.

6 Zusammenfassung (German Summary)

Hintergrund:

Untersuchung des Einflusses von Vitrektomgröße und Schnittrate auf das Überleben gesunder Lymphozyten und Lymphomzellen während diagnostischer Vitrektomien in einem In-vitro-Modell.

Methoden:

Im ersten Experiment wurden gesunde Lymphozyten aus Blutproben einer gesunden Person isoliert. Im zweiten Experiment kamen kultivierte *MYD88*-positive Lymphomzellen einer kommerziellen Zelllinie zum Einsatz. Zellsuspensionen mit definierten Konzentrationen (1×10^3 Zellen/ml, 1×10^4 Zellen/ml und 1×10^6 Zellen/ml) wurden unter kontrollierten Bedingungen vitrektomiert – variiert wurde die Schnittraten (0/min, 1500/min und 5000/min) und Vitrektomgrößen (20G, 23G, 25G und 27G). Für jede Bedingung wurden drei technische Replikate durchgeführt. Die Zellintegrität wurde mittels Durchflusszytometrie (FACS) analysiert. Statistische Signifikanz zwischen den Gruppen wurde mit dem Kruskal-Wallis-Test bestimmt.

Ergebnisse:

Bei gesunden Lymphozyten zeigte sich keine Korrelation zwischen Überlebensrate und Vitrektomgröße oder niedrigeren Schnittraten. Für Lymphomzellen wurde jedoch eine signifikante negative Korrelation zwischen Vitrektomgröße und Zellüberleben festgestellt (Kendalls Tau $\tau = -0{,}253$; $p = 0{,}00048$; Kruskal-Wallis $\chi^2 = 13{,}337$; $p = 0{,}00396$).

Schlussfolgerung:

Größere Vitrektomlumen-Durchmesser korrelierten in unserer Studie mit höheren Überlebensraten von Lymphomzellen. Dies legt nahe, dass eine schonende Vitrektomietechnik bei der Glaskörperbiopsie die diagnostische zelluläre Ausbeute und damit Diagnostik von vitreoretinalen Lymphomen verbessern kann.

Schlüsselwörter: Vitrektomie, Gauge, Schnittrate, vitreoretinales Lymphom, Glaskörperbiopsie, Lymphozyten, Lymphozytenüberleben, FACS.

7 References

Ahmed, A. H., Foster, C. S., & Shields, C. L. (2017). Association of Disease Location and Treatment With Survival in Diffuse Large B-Cell Lymphoma of the Eye and Ocular Adnexal Region. *JAMA ophthalmology*, *135*(10), 1062-1068. https://doi.org/10.1001/jamaophthalmol.2017.3286

Alaggio, R., Amador, C., Anagnostopoulos, I., Attygalle, A. D., Araujo, I. B. O., Berti, E., Bhagat, G., Borges, A. M., Boyer, D., Calaminici, M., Chadburn, A., Chan, J. K. C., Cheuk, W., Chng, W. J., Choi, J. K., Chuang, S. S., Coupland, S. E., Czader, M., Dave, S. S., . . . Xiao, W. (2022). The 5th edition of the World Health Organization Classification of Haematolymphoid Tumours: Lymphoid Neoplasms. *Leukemia*, *36*(7), 1720-1748. https://doi.org/10.1038/s41375-022-01620-2

Alfaar, A. S., Yousef, Y. A., M, W. W., Hassanain, O., Kakkassery, V., Moustafa, M., Kunbaz, A., Esmael, A., & Strauß, O. (2024). Declining incidence and improving survival of ocular and orbital lymphomas in the US between 1995 and 2018. *Sci Rep*, *14*(1), 7886. https://doi.org/10.1038/s41598-024-58508-7

Almeida, D. R., Chin, E. K., Shah, S. S., Bakall, B., Gehrs, K. M., Boldt, H. C., Russell, S. R., Folk, J. C., & Mahajan, V. B. (2016). Comparison of microbiology and visual outcomes of patients undergoing small-gauge and 20-gauge vitrectomy for endophthalmitis. *Clin Ophthalmol*, *10*, 167-172. https://doi.org/10.2147/opth.S95906

Androudi, S., Apivatthakakul, A., Arevalo, F. J., Berkenstock, M. K., Carreño, E., Chee, S.-P., Choovuthayakorn, J., Cimino, L., Cornish, E. E., Farrall, A. L., Gehl, Z., Gentile, P., Gerges, T. K., Gozzi, F., Hernández-Pons, A., Issa, S., Kim, H. M., Kim, M., Knickelbein, J. E., . . . Younan, C. (2024). Presentation, Diagnostic Testing and Initial Treatment of Vitreoretinal Lymphoma. *Ophthalmology Retina*, *8*(1), 72-80. https://doi.org/https://doi.org/10.1016/j.oret.2023.08.012

Arai, A., Takase, H., Yoshimori, M., Yamamoto, K., Mochizuki, M., & Miura, O. (2020). Gene expression profiling of primary vitreoretinal lymphoma. *Cancer Sci*, *111*(4), 1417-1421. https://doi.org/10.1111/cas.14347

Bonzheim, I., Giese, S., Deuter, C., Süsskind, D., Zierhut, M., Waizel, M., Szurman, P., Federmann, B., Schmidt, J., Quintanilla-Martinez, L., Coupland, S. E., Bartz-Schmidt, K. U., & Fend, F. (2015). High frequency of MYD88 mutations in vitreoretinal B-cell lymphoma: a valuable tool to improve diagnostic yield of vitreous aspirates. *Blood*, *126*(1), 76-79. https://doi.org/https://doi.org/10.1182/blood-2015-01-620518

Bonzheim, I., Salmerón-Villalobos, J., Süsskind, D., Szurman, P., Gekeler, F., Spitzer, M. S., Salaverria, I., Campo, E., Coupland, S. E., Quintanilla-Martinez, L., & Fend, F. (2023). [Molecular diagnostics for vitreoretinal lymphoma]. *Pathologie (Heidelb)*, *44*(Suppl 3), 150-154. https://doi.org/10.1007/s00292-023-01251-z (Molekulare Diagnostik des vitreoretinalen Lymphoms.)

Bonzheim, I., Sander, P., Salmerón-Villalobos, J., Süsskind, D., Szurman, P., Gekeler, F., Spitzer, M. S., Steinhilber, J., Kohler, E., Büssgen, M., Schittenhelm, J., Salaverria, I., Campo, E., Coupland, S. E., Quintanilla-Martinez, L., & Fend, F. (2022). The molecular hallmarks of primary and secondary vitreoretinal lymphoma. *Blood Advances*, *6*(5), 1598-1607. https://doi.org/10.1182/bloodadvances.2021004212

Camacho-Fernández, C., Hervás, D., Rivas-Sendra, A., Marín, M. P., & Seguí-Simarro, J. M. (2018). Comparison of six different methods to calculate cell densities. *Plant Methods*, *14*, 30. https://doi.org/10.1186/s13007-018-0297-4

Cani, A. K., Hovelson, D. H., Demirci, H., Johnson, M. W., Tomlins, S. A., & Rao, R. C. (2017). Next generation sequencing of vitreoretinal lymphomas from small-volume intraocular liquid biopsies: new routes to targeted therapies. *Oncotarget*, *8*(5), 7989-7998. https://doi.org/10.18632/oncotarget.14008

Cao, X., Shen, D., Callanan, D. G., Mochizuki, M., & Chan, C.-C. (2011). Diagnosis of systemic metastatic retinal lymphoma. *Acta Ophthalmologica*, *89*(2), e149-e154. https://doi.org/https://doi.org/10.1111/j.1755-3768.2009.01797.x

Carbonell, D., Mahajan, S., Chee, S.-P., Sobolewska, B., Agrawal, R., Bülow, T., Gupta, V., Jones, N. P., Accorinti, M., & Agarwal, M. (2021). Consensus recommendations for the diagnosis of vitreoretinal lymphoma. *Ocular Immunology and Inflammation*, *29*(3), 507-520.

Cassoux, N., Merle-Beral, H., Leblond, V., Bodaghi, B., Miléa, D., Gerber, S., Fardeau, C., Reux, I., Xuan, K. H., Chan, C. C., & LeHoang, P. (2000). Ocular and central nervous system lymphoma: clinical features and diagnosis. *Ocul Immunol Inflamm*, *8*(4), 243-250. https://doi.org/10.1076/ocii.8.4.243.6463

Chan, C. C., Rubenstein, J. L., Coupland, S. E., Davis, J. L., Harbour, J. W., Johnston, P. B., Cassoux, N., Touitou, V., Smith, J. R., & Batchelor, T. T. (2011). Primary vitreoretinal lymphoma: a report from an international primary central nervous system lymphoma collaborative group symposium. *The oncologist*, *16*(11), 1589-1599.

Chan, C. C., & Sen, H. N. (2013). Current concepts in diagnosing and managing primary vitreoretinal (intraocular) lymphoma. *Discov Med*, *15*(81), 93-100.

Choo, C., Cote, O., Bostwick, K., Regueiro, M., Wells, J., Grossniklaus, H. E., Gonzales, J., Yeh, S., Hinterwirth, A., Doan, T., & Shantha, J. G. (2024). Deep sequencing as a diagnostic tool in patients with suspected primary vitreoretinal lymphoma. *Br J Ophthalmol*, *109*(1), 70-75. https://doi.org/10.1136/bjo-2023-324769

Cooper, E. L., & Riker, J. L. (1951). Malignant lymphoma of the uveal tract. *Am J Ophthalmol*, *34*(8), 1153-1158. https://doi.org/10.1016/0002-9394(51)90691-5

Cossarizza, A., Chang, H.-D., Radbruch, A., Akdis, M., Andrä, I., Annunziato, F., Bacher, P., Barnaba, V., Battistini, L., Bauer, W. M., Baumgart, S., Becher, B., Beisker, W., Berek, C., Blanco, A., Borsellino, G., Boulais, P. E., Brinkman, R. R., Büscher, M., . . . Zimmermann, J. (2017). Guidelines

for the use of flow cytometry and cell sorting in immunological studies. *European Journal of Immunology*, *47*(10), 1584-1797. https://doi.org/https://doi.org/10.1002/eji.201646632
Coupland, S. E. (2012). Analysis of intraocular biopsies. *Current Concepts in Uveal Melanoma*, *49*, 96-116.
Coupland, S. E., Chan, C. C., & Smith, J. (2009). Pathophysiology of retinal lymphoma. *Ocular Immunology and Inflammation*, *17*(4), 227-237.
Coupland, S. E., & Damato, B. (2008). Understanding intraocular lymphomas. *Clin Exp Ophthalmol*, *36*(6), 564-578. https://doi.org/10.1111/j.1442-9071.2008.01843.x
Coupland, S. E., Heimann, H., & Bechrakis, N. E. (2004). Primary intraocular lymphoma: a review of the clinical, histopathological and molecular biological features. *Graefes Arch Clin Exp Ophthalmol*, *242*(11), 901-913. https://doi.org/10.1007/s00417-004-0973-0
Dalal, M., Casady, M., Moriarty, E., Faia, L., Nussenblatt, R., Chan, C.-C., & Sen, H. N. (2014). Diagnostic procedures in vitreoretinal lymphoma. *Ocular Immunology and Inflammation*, *22*(4), 270-276.
Dawson, A. C., Williams, K. A., Appukuttan, B., & Smith, J. R. (2018). Emerging diagnostic tests for vitreoretinal lymphoma: a review. *Clinical & Experimental Ophthalmology*, *46*(8), 945-954. https://doi.org/https://doi.org/10.1111/ceo.13304
de Oliveira, P. R., Berger, A. R., & Chow, D. R. (2016). Vitreoretinal instruments: vitrectomy cutters, endoillumination and wide-angle viewing systems. *Int J Retina Vitreous*, *2*, 28. https://doi.org/10.1186/s40942-016-0052-9
Denniston, A. K., & Keane, P. A. (2015). Paravascular Pathways in the Eye: Is There an 'Ocular Glymphatic System'? *Investigative Ophthalmology & Visual Science*, *56*(6), 3955-3956. https://doi.org/10.1167/iovs.15-17243
Fadlelseed, H., Rhatigan, M., Treacy, M., Murphy, C., O'Neill, J., Kilmartin, D., & Kennedy, S. (2024). Vitreoretinal large B- cell lymphoma (VR- LBCL): Clinical and pathological features and treatment outcomes. *Pathology - Research and Practice*, *261*, 155500. https://doi.org/https://doi.org/10.1016/j.prp.2024.155500
Fardeau, C., Lee, C. P., Merle-Béral, H., Cassoux, N., Bodaghi, B., Davi, F., & Lehoang, P. (2009). Retinal fluorescein, indocyanine green angiography, and optic coherence tomography in non-Hodgkin primary intraocular lymphoma. *American journal of ophthalmology*, *147*(5), 886-894. e881.
Farrall, A. L., & Smith, J. R. (2023). Incidence and survival of ocular diffuse large B-cell lymphomas. *Acta Ophthalmol*, *101*(3), e353-e354. https://doi.org/10.1111/aos.15284
Fend, F., Ferreri, A. J. M., & Coupland, S. E. (2016). How we diagnose and treat vitreoretinal lymphoma. *British Journal of Haematology*, *173*(5), 680-692. https://doi.org/https://doi.org/10.1111/bjh.14025
Fox, R. W., & McDonald, A. T. (1995). *Introduction to Fluid Mechanics: SI Version*. J. Wiley.
Giuffrè, C., Menean, M., Modorati, G. M., Marchese, A., Cicinelli, M. V., Bandello, F., & Miserocchi, E. (2020). Primary vitreoretinal lymphoma:

recent advances and literature review. *Annals of Lymphoma*, *4*. https://aol.amegroups.org/article/view/6843
Gonzales, J. A., & Chan, C.-C. (2007). Biopsy techniques and yields in diagnosing primary intraocular lymphoma. *International ophthalmology*, *27*, 241-250.
Hiemcke-Jiwa, L. S., Ten Dam-van Loon, N. H., Leguit, R. J., Nierkens, S., Ossewaarde-van Norel, J., de Boer, J. H., Roholl, F. F., de Weger, R. A., Huibers, M. M. H., de Groot-Mijnes, J. D. F., & Kuiper, J. J. W. (2018). Potential Diagnosis of Vitreoretinal Lymphoma by Detection of MYD88 Mutation in Aqueous Humor With Ultrasensitive Droplet Digital Polymerase Chain Reaction. *JAMA Ophthalmol*, *136*(10), 1098-1104. https://doi.org/10.1001/jamaophthalmol.2018.2887
Huang, R. S., Mihalache, A., Popovic, M. M., Cruz-Pimentel, M., Pandya, B. U., Muni, R. H., & Kertes, P. J. (2024). Diagnostic methods for primary vitreoretinal lymphoma: A systematic review. *Survey of Ophthalmology*, *69*(3), 456-464. https://doi.org/https://doi.org/10.1016/j.survophthal.2023.12.001
Hwang, C. S., Yeh, S., & Bergstrom, C. S. (2014). Diagnostic vitrectomy for primary intraocular lymphoma: when, why, how? *Int Ophthalmol Clin*, *54*(2), 155-171. https://doi.org/10.1097/iio.0000000000000022
Iliff, J. J., Wang, M., Liao, Y., Plogg, B. A., Peng, W., Gundersen, G. A., Benveniste, H., Vates, G. E., Deane, R., Goldman, S. A., Nagelhus, E. A., & Nedergaard, M. (2012). A paravascular pathway facilitates CSF flow through the brain parenchyma and the clearance of interstitial solutes, including amyloid β. *Sci Transl Med*, *4*(147), 147ra111. https://doi.org/10.1126/scitranslmed.3003748
Jiang, T., Zhao, Z., & Chang, Q. (2014). Evaluation of cytologic specimens obtained during experimental vitreous biopsy using B-cell lymphoma line. *European Journal of Ophthalmology*, *24*(6), 911-917.
Kanavi, M. R., Soheilian, M., Hosseini, S. B., & Azari, A. A. (2014). 25-gauge transconjunctival diagnostic vitrectomy in suspected cases of intraocular lymphoma: a case series and review of the literature. *International journal of ophthalmology*, *7*(3), 577.
Kizhakeyil, A., Ong, S. T., Fazil, M., Chalasani, M. L. S., Prasannan, P., & Verma, N. K. (2019). Isolation of Human Peripheral Blood T-Lymphocytes. *Methods Mol Biol*, *1930*, 11-17. https://doi.org/10.1007/978-1-4939-9036-8_2
Küppers, R. (2005). Mechanisms of B-cell lymphoma pathogenesis. *Nat Rev Cancer*, *5*(4), 251-262. https://doi.org/10.1038/nrc1589
Kwak, J. J., Lee, K. S., Lee, J., Kim, Y. J., Choi, E. Y., Byeon, S. H., Chang, W. S., Kim, Y. R., Kim, J. S., Shin, S., Lee, S. T., Kim, S. S., & Lee, C. S. (2023). Next-Generation Sequencing of Vitreoretinal Lymphoma by Vitreous Liquid Biopsy: Diagnostic Potential and Genotype/Phenotype Correlation. *Invest Ophthalmol Vis Sci*, *64*(14), 27. https://doi.org/10.1167/iovs.64.14.27
Lee, D., Lee, J., Nahm, J.-H., & Kim, M. (2022). Diagnostic Accuracy of Vitreous Cytology in Patients with Vitreoretinal Lymphoma. *Journal of Clinical Medicine*, *11*(21), 6450. https://www.mdpi.com/2077-0383/11/21/6450

Levasseur, S. D., Wittenberg, L. A., & White, V. A. (2013). Vitreoretinal lymphoma: a 20-year review of incidence, clinical and cytologic features, treatment, and outcomes. *JAMA ophthalmology*, *131*(1), 50-55.

Levin, L. A., Nilsson, S. F., Ver Hoeve, J., Wu, S., Kaufman, P. L., & Alm, A. (2011). *Adler's Physiology of the Eye: Expert Consult-Online and Print*. Elsevier Health Sciences.

Magalhaes, O., Jr., Chong, L., DeBoer, C., Bhadri, P., Kerns, R., Barnes, A., Fang, S., & Humayun, M. (2008). Vitreous dynamics: vitreous flow analysis in 20-, 23-, and 25-gauge cutters. *Retina*, *28*(2), 236-241. https://doi.org/10.1097/IAE.0b013e318158e9e0

Magalhaes, O., Jr., Maia, M., Rodrigues, E. B., Machado, L., Costa, E. F., Maia, A., Moares-Filho, M. N., Dib, E., & Farah, M. E. (2011). Perspective on fluid and solid dynamics in different pars plana vitrectomy systems. *Am J Ophthalmol*, *151*(3), 401-405 e401. https://doi.org/10.1016/j.ajo.2010.11.009

Mahajan, V. B., Tarantola, R. M., Graff, J. M., Boldt, H. C., Abramoff, M. D., Russell, S. R., & Folk, J. C. (2011). Sutureless triplanar sclerotomy for 23-gauge vitrectomy. *Arch Ophthalmol*, *129*(5), 585-590. https://doi.org/10.1001/archophthalmol.2011.101

Malinowski, S. M. (2010). The vitreous trap: a simple, surgeon-controlled technique for obtaining undiluted vitreous and subretinal specimens during pars plana vitrectomy. *Retina*, *30*(5), 828-829.

McKinnon, K. M. (2018). Flow Cytometry: An Overview. *Current Protocols in Immunology*, *120*(1), 5.1.1-5.1.11. https://doi.org/https://doi.org/10.1002/cpim.40

Melli, B., Gentile, P., Nicoli, D., Farnetti, E., Croci, S., Gozzi, F., Bolletta, E., De Simone, L., Sanguedolce, F., Palicelli, A., Zizzo, M., Ricci, S., Ilariucci, F., Rossi, C., Cavazza, A., Ascani, S., Cimino, L., & Zanelli, M. (2022). Primary Vitreoretinal Lymphoma: Current Diagnostic Laboratory Tests and New Emerging Molecular Tools. *Curr Oncol*, *29*(10), 6908-6921. https://doi.org/10.3390/curroncol29100543

Menean, M., Giuffrè, C., Cicinelli, M. V., Marchese, A., Modorati, G., Bandello, F., & Miserocchi, E. (2023). A comprehensive overview of diagnosis, imaging and treatment of vitreoretinal lymphoma. *European Journal of Ophthalmology*, *0*(0), 11206721231211931. https://doi.org/10.1177/11206721231211931

Mohamed, S., Claes, C., & Tsang, C. W. (2017). Review of Small Gauge Vitrectomy: Progress and Innovations. *J Ophthalmol*, *2017*, 6285869. https://doi.org/10.1155/2017/6285869

Pandit, S., Modi, Y., & Mehta, N. (2023). Advances in Vitrectomy. In E. Tsui, S. S. M. Fung, & R. B. Singh (Eds.), *Current Advances in Ocular Surgery* (pp. 313-324). Springer Nature Singapore. https://doi.org/10.1007/978-981-99-1661-0_17

Qualman, S. J., Mendelsohn, G., Mann, R. B., & Green, W. R. (1983). Intraocular lymphomas. Natural history based on a clinicopathologic study of eight cases and review of the literature. *Cancer*, *52*(5), 878-886. https://doi.org/10.1002/1097-0142(19830901)52:5<878::aid-cncr2820520523>3.0.co;2-d

Ribeiro, L., Oliveira, J., Kuroiwa, D., Kolko, M., Fernandes, R., Junior, O., Moraes, N., Vasconcelos, H., Oliveira, T., & Maia, M. (2022). Advances in Vitreoretinal Surgery. *J Clin Med*, *11*(21). https://doi.org/10.3390/jcm11216428

Roizenblatt, M., Edwards, T. L., & Gehlbach, P. L. (2018). Robot-assisted vitreoretinal surgery: current perspectives. *Robot Surg*, *5*, 1-11. https://doi.org/10.2147/rsrr.S122301

Sadeghi, E., Mohan, S., Iannetta, D., & Chhablani, J. (2023). Recent developments in imaging and surgical vision technologies currently available for improving vitreoretinal surgery: a narrative review. *Expert Rev Med Devices*, *20*(8), 651-672. https://doi.org/10.1080/17434440.2023.2231841

Sebag, J. (1987). Structure, function, and age-related changes of the human vitreous. *Bull Soc Belge Ophtalmol*, *223 Pt 1*, 37-57. https://doi.org/10.1007/978-1-4757-1901-7_3

Sebag, J. (2016). *Vitreous*. Springer.

Seifert, M., Scholtysik, R., & Küppers, R. (2013). Origin and pathogenesis of B cell lymphomas. *Methods Mol Biol*, *971*, 1-25. https://doi.org/10.1007/978-1-62703-269-8_1

Shaffer, A. L., 3rd, Young, R. M., & Staudt, L. M. (2012). Pathogenesis of human B cell lymphomas. *Annu Rev Immunol*, *30*, 565-610. https://doi.org/10.1146/annurev-immunol-020711-075027

Singh, A. D., & Damato, B. E. (2019). *Clinical ophthalmic oncology: basic principles*. Springer.

Sjö, L. D. (2009). Ophthalmic lymphoma: epidemiology and pathogenesis. *Acta Ophthalmol*, *87 Thesis 1*, 1-20. https://doi.org/10.1111/j.1755-3768.2008.01478.x

Snell, R. S., & Lemp, M. A. (2013). *Clinical anatomy of the eye*. John Wiley & Sons.

Sobolewska, B., Chee, S. P., Zaguia, F., Goldstein, D. A., Smith, J. R., Fend, F., Mochizuki, M., & Zierhut, M. (2021). Vitreoretinal Lymphoma. *Cancers (Basel)*, *13*(16). https://doi.org/10.3390/cancers13163921

Soussain, C., Malaise, D., & Cassoux, N. (2021). Primary vitreoretinal lymphoma: a diagnostic and management challenge. *Blood*, *138*(17), 1519-1534. https://doi.org/https://doi.org/10.1182/blood.2020008235

Takase, H., Arai, A., Iwasaki, Y., Imai, A., Nagao, T., Kawagishi, M., Ishida, T., & Mochizuki, M. (2022). Challenges in the diagnosis and management of vitreoretinal lymphoma - Clinical and basic approaches. *Prog Retin Eye Res*, *90*, 101053. https://doi.org/10.1016/j.preteyeres.2022.101053

Tan, W. J., Wang, M. M., Ricciardi-Castagnoli, P., Chan, A. S. Y., & Lim, T. S. (2020). Cytologic and Molecular Diagnostics for Vitreoretinal Lymphoma: Current Approaches and Emerging Single-Cell Analyses. *Front Mol Biosci*, *7*, 611017. https://doi.org/10.3389/fmolb.2020.611017

Tang, P. H., Karkhur, S., & Nguyen, Q. D. (2020). Obtaining undiluted vitreous sample using small gauge pars plana vitrectomy and air infusion. *American Journal of Ophthalmology Case Reports*, *19*, 100768.

Tarantola, R. M., Graff, J. M., Somani, R., & Mahajan, V. B. (2012). Temporal approach for small-gauge pars plana vitrectomy combined with anterior

segment surgery. *Retina*, *32*(8), 1614-1623. https://doi.org/10.1097/IAE.0b013e318244536f
Team, R. C. (2024). *R: A language and environment for statistical computing*. In R Foundation for Statistical Computing. https://www.R-project.org/
Tekumalla, S., Xu, D., Awh, K., Philp, N., Milman, T., & Garg, S. (2023). Diagnostic Yield of in Vitro Vitreous Biopsy for Intraocular Lymphoma at Variable Vitreous Cutter Speeds Using 25-Gauge Vitrectomy. *Retina*, *43*(6), 1005-1009. https://doi.org/10.1097/IAE.0000000000003753
Thurner, L., Hartmann, S., Neumann, F., Hoth, M., Stilgenbauer, S., Küppers, R., Preuss, K.-D., & Bewarder, M. (2020). Role of Specific B-Cell Receptor Antigens in Lymphomagenesis [Review]. *Frontiers in Oncology*, *10*. https://doi.org/10.3389/fonc.2020.604685
Touitou, V., Daussy, C., Bodaghi, B., Camelo, S., de Kozak, Y., Lehoang, P., Naud, M. C., Varin, A., Thillaye-Goldenberg, B., Merle-Béral, H., Fridman, W. H., Sautès-Fridman, C., & Fisson, S. (2007). Impaired th1/tc1 cytokine production of tumor-infiltrating lymphocytes in a model of primary intraocular B-cell lymphoma. *Invest Ophthalmol Vis Sci*, *48*(7), 3223-3229. https://doi.org/10.1167/iovs.07-0008
Uddin, N., & Rutar, M. (2022). Ocular Lymphatic and Glymphatic Systems: Implications for Retinal Health and Disease. *Int J Mol Sci*, *23*(17). https://doi.org/10.3390/ijms231710139
Ulltang, E., Kiilgaard, J. F., Mola, N., Scheie, D., Heegaard, S., & Krohn, J. (2021). Vitrectomy-Assisted Biopsy: An in vitro Study on the Impact of Cut Rate and Probe Size. *Ocul Oncol Pathol*, *7*(5), 346-352. https://doi.org/10.1159/000516960
Venkatesh, R., Bavaharan, B., Mahendradas, P., & Yadav, N. K. (2019). Primary vitreoretinal lymphoma: prevalence, impact, and management challenges. *Clin Ophthalmol*, *13*, 353-364. https://doi.org/10.2147/opth.S159014
Wittenberg, L. A., Maberley, D. A., Ma, P. E., Wade, N. K., Gill, H., & White, V. A. (2008). Contribution of vitreous cytology to final clinical diagnosis: fifteen-year review of vitreous cytology specimens from one institution. *Ophthalmology*, *115*(11), 1944-1950.
Xu, D., Awh, K., Philp, N., Milman, T., & Garg, S. (2022). Diagnostic Yield of Vitreous Biopsy for Primary Vitreoretinal Lymphoma. *Investigative Ophthalmology & Visual Science*, *63*(7), 3584–A0013-3584–A0013.
Young, R. M., Phelan, J. D., Wilson, W. H., & Staudt, L. M. (2019). Pathogenic B-cell receptor signaling in lymphoid malignancies: New insights to improve treatment. *Immunol Rev*, *291*(1), 190-213. https://doi.org/10.1111/imr.12792

8 Declaration of personal contribution (Eigenanteilserklärung)

Die vorliegende Arbeit wurde in Zusammenarbeit der Universitätsaugenklinik mit der AG Lang der Kinderklinik und dem Institut für Pathologie am Universitätsklinikum Tübingen unter Betreuung von Prof. Dr. Karl-Ulrich Bartz-Schmidt durchgeführt.

Die anfängliche Planung und Konzeption der Experimente erfolgte gemeinsam mit Frau Dr. Friederike Kortüm (Betreuerin) und Herrn Prof. Dr. Karl-Ulrich Bartz.-Schmidt (Doktorvater). Die Konzeption und Einarbeitung in alle labortechnischen Methoden erfolgte durch Herrn Florian Heubach und Frau Roksana Wojcik.

Die Versuche wurden nach der Einarbeitung durch Herrn Heubach, Frau Wojcik und Frau Kortüm von mir eigenständig durchgeführt, ebenso die Datenauswertung und -interpretation.

Die statistische Auswertung erfolgte nach einer Beratung durch das Institut für Biometrie eigenständig durch mich.

Ich versichere, das Manuskript selbständig verfasst zu haben und keine weiteren als die von mir angegebenen Quellen verwendet zu haben.

9 Publications

Kowalski M., Bartz-Schmidt KU., Merle DA., Kakkassery V, Heubach F, Athanasiou A, Dimopoulos S, Paigin S, Fend F, Kortuem FC. (2025) DECODE VRL Report No. 1: Lymphocyte survival after diagnostic vitrectomy - does size matter? *Transl Vis Sci Tech.* 2025.

10 Acknowledgements

I would like to express my sincere gratitude to all those who have supported me throughout my doctoral journey. First and foremost, I extend my deepest appreciation to my doctoral supervisor, Prof. Karl-Ulrich Bartz-Schmidt, for his invaluable guidance, support, and profound expertise. His mentorship has been instrumental in shaping both this thesis and my clinical growth as an ophthalmologist.

I am equally indebted to Dr. Friederike Kortüm, whose supervision, insights, and encouragement have been pivotal to the success of this work. Her dedication and expertise have been a valuable guidance throughout this process.

My heartfelt thanks go to my collaborators from AG Lang, particularly Florian Heubach and Roksana Wojcik, without whose contributions this work would not have been feasible. I am also grateful to our partners at the Institute of Pathology, especially Prof. Fend and Stephanie Paigin, for providing the lymphoma cell cultures that were crucial to our research.

I would like to express my gratitude for the support and even friendship of my colleagues, professors and fellow residents at the University Eye Clinic Tübingen. The following deserve special mention: Dr. Michael Birk, Dr. David Merle, Dr. Sven Schnichels, Dr. Torsten Straßer and Prof. Sebastian Thaler. Their friendship, intellectual discussions, and collaborative spirit have made this journey both enjoyable and intellectually stimulating.

My sincere appreciation goes to the Institute for Clinical Epidemiology and Applied Biometry at the University of Tübingen for their expert consulting advice in the field of statistics. Their guidance has been instrumental in ensuring the robustness of our research methodology and findings.

Finally, I wish to express my profound gratitude to my beloved parents and family for their consistent support and encouragement, which have been essential to my perseverance. From the beginning of my studies to the completion of this thesis,

they have been pillars of strength, providing emotional support during challenging times and celebrating every milestone along the way. Their sacrifices and unconditional love have been a driving force behind my academic pursuits, and I am forever indebted to them for helping me to grow and realize my potentials.

This journey would not have been possible without the collective support of all these individuals and institutions. Their contributions, both big and small, have shaped not only this thesis but also my growth as a researcher, clinician and an individual. I am profoundly grateful for the opportunity to have worked alongside such brilliant and supportive people, and I look forward to carrying the lessons learned and relationships forged during this journey into my future endeavours.